AD NUMBER

AD010759

NEW LIMITATION CHANGE

TO

Approved for public release, distribution unlimited

FROM

Distribution authorized to U.S. Gov't. agencies and their contractors; Administrative/Operational Use; 31 DEC 1952. Other requests shall be referred to Office of Naval Research, Arlington, VA 22203.

AUTHORITY

ONR ltr dtd 9 Nov 1977

AD- 10759

UNCLASSIFIED

BROWN UNIVERSITY

ONR Contract N6ori-88, T. O. I.

NR-019-102

Technical Report No. 20

I. BOND MOMENTS AND DERIVATIVES IN SiF_4, CF_4, A

SF_6 FROM INFRARED INTENSITIES

By

P. N. Schatz and D. F. Hornig

II. THE DESIGN OF PHOTOELECTRIC RAMAN APPARATUS

By

William R. Busing

III. THE VIBRATIONAL SPECTRA OF MOLECULES AND COMPLEX IONS IN CRYSTALS. VI. CARBON DIOXIDE

By

W. E. Osberg and D. F. Hornig

Metcalf Research Laboratory
Brown University
Providence, Rhode Island

31 December 1952

ABSTRACT

The absolute intensities of the fundamental infrared absorption bands of SiF_4, CF_4 and SF_6 were measured utilizing the pressure broadening technique. The effective bond moments, μ_o, and bond moment derivatives are calculated as a function of the most general potential constants. The most probable values, based on a valence force field plus repulsion between non-bonded atoms (~~first~~ second column) and the alternative (~~second~~ first column), are as follows:

SiF_4	μ_o = 3.3 d	2.3 d
	$\partial\mu/\partial r$ = 3.66 d/A	-7.49 d/A
CF_4	μ_o = 2.36 d	1.12 d
	$\partial\mu/\partial r$ = 3.35 d/A	4.88 d/A
SF_6	μ_o = 0.65 d	2.65 d
	$\partial\mu/\partial r$ = - 6.58 d/A	3.85 d/A

The results are discussed.

BOND MOMENTS AND DERIVATIVES IN CF_4, SiF_4, and SF_6 FROM INFRARED INTENSITIES

P. N. Schatz and D. F. Hornig

Metcalf Chemical Laboratories, Brown University, Providence, R. I.

INTRODUCTION

This paper reports the absolute infrared intensities of the fundamental vibrations of three fluorine containing molecules and some properties of bonds to fluorine inferred from these measurements. In particular, the bond moment and its derivatives with respect to interatomic distance have been calculated for the compounds investigated.

A considerable amount of work has been done in the past several years on the measurement and interpretation of the absolute intensities of infrared bands. The results have usually been interpreted on the basis of molecules composed of non-interacting bond dipole moments, it being assumed that the change in moment during stretching is directed along the bond and that during bending perpendicular to it. The fact that the same bond moment calculated from different modes of vibration sometimes has significantly different values (e.g., in ethylene[1])

---

1. A. M. Thorndike, A. J. Wells, and E. B. Wilson, Jr., J. Chem. Phys. 15, 157 (1947)

---

indicates that this simple model is not always satisfactory. Nevertheless, such a model has given valuable information about the charge distributions in molecules and was employed in this present work.

One of the effects which can cause the preceding assumptions to break down is the polarization of one bond by another. In this respect fluorine compounds constitute a relatively favorable case. The polarizability of a bond is measured by the refraction, which is generally small in bonds to fluorine, being about the same as the C-H and C-C bonds, but considerably smaller than multiple bonds or other halogen bonds. (For example[2],

2. C. P. Smyth, Phil. Mag. 50, 361 (1925)

C-H, 1.7; C-C, 1.2; C-F, 1.6; S-F, 2.0; but C=C, 4.2; C-Cl, 6.6). Consequently, it is hoped that the polarization interactions among the various bonds were kept to a minimum. Of course, hybridization changes during a vibration may still cause large interaction effects.

BASIC THEORY

The experimentally observed absolute intensity, A, is related to the absorption coefficient α_ν by

$$A = \int_{\text{Band}} \alpha_\nu \, d\nu = \frac{1}{p\ell}\int \ln \frac{I_o}{I} \, d\nu \, , \qquad (1)$$

where p is the partial pressure of absorbing gas, ℓ is the path length of the cell, I_o is the incident intensity of radiation of frequency ν and I is the transmitted intensity. It has been shown that[3]

3. B. L. Crawford, Jr., and H. L. Dinsmore, J. Chem. Phys. 18, 983, 1682 (1950).

$$A_i^{i'} = \left(\frac{8\pi^3 \nu_i^{i'}}{3 h c}\right)\left(\frac{N_i}{g_i}\right)\left[1 - \exp\left(-\frac{h \nu_i^{i'}}{k T}\right)\right] S_i^{i'} , \quad (2)$$

where $\nu_i^{i'}$ is the frequency corresponding to the transition between the energy levels i and i', N_i is the population of the energy level i, and g_i is its multiplicity. $S_i^{i'}$ is known as the line strength and is defined by

$$S_i^{i'} = \sum_{a_i, a_i'} \left| (i \,|\, \underline{p} \,|\, i') \right|^2 , \quad (3)$$

the summation being carried out over all the individual degenerate states a_i and a_i'. $\underline{p}$ is the vector dipole moment in a space-fixed coordinate system, and $(i \,|\, \underline{p} \,|\, i')$ is the matrix element of the electric moment between the states i and i'. The integrated intensity of a vibration-rotation band is the sum of expressions (2) for all transitions occurring. Such a summation has been carried out for diatomic molecules[3] (and a closely similar treatment applies to linear molecules[4])

---

4. D. F. Eggers, Jr., and B. L. Crawford, Jr., J. Chem. Phys. 19, 1554 (1951)

---

and is readily extended to spherical top molecules. Assuming as a first approximation that the rotational and vibrational wave functions are separable, and that the electronic wave function remains constant for transitions giving rise to absorption in the infrared region, the line strength $S_i^{i'}$ may be expressed as a product of rotational and vibrational line strengths[3];

$$S_i^{i'} = S_r^{r'} \, S_v^{v'} . \quad (4)$$

To this degree of approximation, the vibrational wave function can be expressed as a product of independent harmonic oscillator wave functions, one corresponding to each normal mode of vibration. The energy levels corresponding to any particular mode of vibration are given by,

$$E_v = \left(v + \tfrac{1}{2} \right) h \nu_o \qquad (5)$$

where v is an integer and ν_o is the classical frequency of vibration.

The eigenvalues and eigenfunctions of the symmetric top (of which the spherical top is a special case) are well known[5].

---

5. F. Reichle and R. Rademacher, Zeits. f. Physik 39, 444 (1926)

The rotational energy levels of a spherical top are given by,

$$E_j = \frac{h^2}{8\pi^2 A} \; j\,(j+1), \qquad (6)$$

where A is the principal moment of inertia and j is an integer. There is a $(2j+1)^2$-fold degeneracy corresponding to any given value of j, since every level has a $(2j+1)$-fold degeneracy because j may have $(2j+1)$ orientations with respect to a fixed direction in the molecule (quantum number k) in addition to the usual $(2j+1)$-fold space degeneracy (quantum number m).

The expression for the total intensity corresponding to any given vibrational transition, $A_v^{v'}$, is obtained by summing the expression for $A_i^{i'}$ over all transitions occurring in the band. Making

use of Boltzmann statistics and using equation (4) yields,

$$A_v^{v'} = \frac{8\pi^3 N_v}{3hcZ} S_v^{v'} \sum_{r,r'} \nu_{vj}^{v'j'} \left(1 - \exp\left(\frac{h\nu_{vj}^{v'j'}}{kT}\right)\right) e^{-E_j/kT} S_r^{r'} \quad (7)$$

where the symbol $\sum_{r,r'}$ indicates a summation over all allowed rotational transitions. N_v is the total molecular concentration in the lower vibrational level and Z is the rotational partition function defined by

$$Z = \sum_{j=0}^{\infty} (2j+1)^2 e^{Ej/kT} \quad (8)$$

The selection rules for the vibration-rotation transitions of a symmetric top are different depending on whether the transition moment is parallel or perpendicular to the figure axis. However, in the case of a spherical top, any axis fixed in the molecule may be considered as the figure axis[6].

---

6. G. Herzberg, Infrared and Raman Spectra of Polyatomic Molecules, D. Van Nostrand Co., 1945, p. 38.

For convenience, then, let the figure axis be chosen so that the transition moment is parallel to it. Then the selection rules are[7],

---

7. Ibid., p. 414.

$$\Delta k = 0, \ \Delta j = 0, \pm 1 \quad \text{if } k \neq 0$$
$$\Delta k = 0, \ \Delta j = \pm 1 \quad \text{if } k = 0 \quad (9)$$

The symbol $\sum_{r,r'}$ appearing in equation (7) is actually a triple sum, since in summing over any j value the two previously mentioned degeneracies must be considered. Hence equation (7) may be written,

$$A_v^{v'} = \frac{8\pi^3 N_v}{3hcZ} S_v^{v'} \sum_{i,j'} \left(\nu_{vj}^{v'j'} e^{-E_j/kT} - e^{-\frac{h\nu_v^{v'}}{kT}} \nu_{vj}^{v'j'} e^{-E_{j'}/kT} \right) \quad (10)$$

$$\times \sum_{k,k'} \sum_{m,m'} S_r^{r'}$$

The summation $\sum_{m,\,m'} S_r^{r'}$ has been carried out by Rademacher and Peichc with the result[8],

---

8. R. Rademacher and F. Reichle, Zeits. f. Physik 41, 453 (1927)

$$\sum_{m,m'} S_r^{r'} = S_{jk}^{j'k'} = \frac{k^2(2j+1)}{j(j+1)} \delta_{j,j'} + \frac{(j+k)(j-k)}{j} \delta_{j,j'-1} \quad (11)$$

$$+ \frac{(j+1+k)(j+1-k)}{(j+1)} \delta_{j,j'+1}$$

It is now necessary to evaluate the sum, $\sum_{k,\,k'} S_j^{j'\,k'}$. Since $k' = k$ (equation (9)), it will merely be necessary to sum the terms corresponding to the $(2j + 1)$ possible orientations allowed for k. This may easily be done if it is noted that

$$\sum_{k=-j}^{k=+j} k^2 = \frac{1}{3} j(j+1)(2j+1) \quad (12)$$

Thus,

$$S_j^{j'} = \sum_{k=-j}^{k=j} S_{jk}^{j'k'} = \frac{1}{3}(2j+1)^2 \delta_{j,j'} + \left(\frac{4}{3} j^2 - \frac{1}{3}\right) \delta_{j,j'-1} \quad (13)$$

$$+ \left(\frac{4}{3} j^2 + \frac{8}{3} j + 1\right) \delta_{j,j'+1}$$

Hence equation (10) becomes

$$A_v^{v'} = \frac{8\pi^3 N_v}{3hcZ} S_v^{v'} \left[\sum_{j,j'} \left(\nu_{vj}^{v'j'} e^{-E_j/kT} S_j^{j'} \right) \right. \quad (14)$$

$$\left. - e^{-\frac{h\nu_v^{v'}}{kT}} \sum_{j,j'} \nu_{vj}^{v'j'} e^{-E_{j'}/kT} S_j^{j'} \right]$$

Summing finally over j' and j yields,

$$A_v^{v'} = \frac{8\pi^3 N_v}{3hc} S_v^{v'} \left[\nu_v^{v'} \left(1 - e^{-\frac{h\nu_v^{v'}}{kT}}\right) + 2B\left(1 + e^{-\frac{h\nu_v^{v'}}{kT}}\right) \right] \quad (15)$$

In order to obtain the total intensity of the band, $A^{(n)}$, $A_v^{v'}$ must be summed over all values of v, and it must be noted that the infrared active vibrations of tetrahedral and octahedral molecule are triply degenerate. That is,

$$A(n) = 3 \sum_{v=0}^{\infty} A_v^{v+n} \quad (16)$$

This summation has been carried out by Crawford and Dinsmore with the result that[3],

$$A^{(n)} = \frac{8\pi^3 N}{nhcQ} S_0^n \left[\nu_0^n \left(1 - e^{-\frac{nh\nu_0}{kT}}\right) + 2B\left(1 + e^{-\frac{nh\nu_0}{kT}}\right) \right] Q^{n+1} \quad (17)$$

where Q is the vibrational partition function and N is the total molecular concentration. For fundamental vibrations n is equal to unity, and for all of the molecules studied in this work the quantity $\frac{2B}{\nu_0^1}$ is extremely small. Therefore,

$$A(1) \equiv A = \frac{8\pi^3 N \nu_0}{hc} S_0^2 \quad (18)$$

It is interesting to note that for fundamental vibrations the effect of induced emission is exactly offset by the sum of the vibrational transitions 1-2, 2-3, 3-4 ..., provided $\frac{2B}{\nu_0^1} \ll 1$.

If the vector dipole moment is expanded in a Taylor's series as a function of the normal coordinates and terms higher than linear are neglected, the quantity S_0' is easily shown to be[1]

$$S_0' = \frac{h}{8\pi^2 \nu_0} \left(\frac{\partial \mu}{\partial Q_i} \right)^2, \quad (19)$$

where Q_i is the normal coordinate for the particular vibration under consideration, and μ is the vector dipole moment of the molecul (coordinates fixed in the molecule). With this result, equation (19) becomes

$$A_i = \frac{N\pi}{c} \left(\frac{\partial \mu}{\partial Q_i}\right)^2 , \qquad (20)$$

$$A_i' = \frac{N\pi}{c^2} \left(\frac{\partial \mu}{\partial Q_i}\right)^2 , \qquad (20')$$

where A_i is the absolute intensity of the i-th rotation-vibration band in cycles/cm atm sec, and A_i' is the same quantity expressed in cm^{-1}/cm atm, if N is the molecular concentration at one atmosphere pressure.

Since Crawford and Dinsmore[3] have shown that higher order effect such as electrical and mechanical anharmonicity produce negligible changes in the intensity of fundamental vibrations they have been ignored.

BOND MOMENTS & DERIVATIVES

In order to obtain information about the individual bonds of a molecule, the relationship between the normal coordinates and internal coordinates must be utilized. If the molecule possesses any symmetry the latter are most conveniently taken as symmetry coordinates which factor the secular determinant. In the three molecul discussed here only one symmetry species (F_2 of T_d, F_{1u} of O_h), can be infrared active; it contains two normal coordinates, Q_1 and Q_2, each a normalized linear combination of two symmetry coordinates, R_1 and R_2. In Wilson's notation[9],

---

9. E. B. Wilson, Jr., J. Chem. Phys. 7, 1047 (1939); 9, 76 (1941)

---

the desired relationship is

$$\frac{\partial \mu}{\partial R_k} = L^{-1}_{1k} \left(\frac{\partial \mu}{\partial Q_1}\right) + L^{-1}_{2k} \left(\frac{\partial \mu}{\partial Q_2}\right) \qquad k = 1,2 \quad , \tag{21}$$

where L^{-1} is the matrix of the transformation $Q = L^{-1} R$. The elements of L^{-1} are given explicitly in terms of Wilson's F (potential energy) and G (kinetic energy) matrices by the expressions

$$\frac{L^{-1}_{i1}}{L^{-1}_{i2}} = - \frac{(GF)_{2i} - \lambda_2 \delta_{2i}}{(GF)_{1i} - \lambda_1 \delta_{1i}} = n_i \qquad i = 1,2 \tag{22}$$

and

$$(L^{-1}_{i2})^{-2} = G_{22} + 2n_i G_{12} + n^2_i G_{11} \qquad i = 1,2 \quad , \tag{23}$$

where δ is the Kronecker symbol and $\lambda_i = 4\pi^2 \nu_i^2$, if ν_i is the frequency of the $i^{\underline{th}}$ normal vibration.

Unfortunately, the force constants, F_{ij}, can only be ascertained by fitting the roots of the secular equation, which for the infrared active species of the molecules studied here is[10]

10. G. Herzberg, Infrared and Raman Spectra of Polyatomic Molecules, D. Van Nostrand Co., 1945.

$$\left\{ \begin{vmatrix} F_{11} & F_{12} \\ F_{12} & F_{22} \end{vmatrix} \begin{vmatrix} G_{11} & G_{12} \\ G_{12} & G_{22} \end{vmatrix} - \begin{vmatrix} \lambda & 0 \\ 0 & \lambda \end{vmatrix} \right\} = 0 \tag{24}$$

Since there are three force constants and but two frequencies, the problem is indeterminate and the best that can be done in the general case, in the absence of precise measurements on isotopic molecules, is to obtain a relation between the three force constants.

A definite solution can, however, be obtained through the use of a physical model which reduces the number of independent constants which must be determined empirically. In the case of a large number of tetrahedral molecules, a model based on the Urey-Bradley field, a simple valence potential plus central forces between non-bonded atoms, has been used successfully by both Heath and Linnett[11],

---

11. J. W. Linnett and D. F. Heath, Trans. Far. Soc. 44, 561, 878, 884 (1948); J. Chem. Phys. 19, 801 (1951)

(3 constants) and Simanouti[12]

---

12. T. Simanouti, J. Chem. Phys. 17, 245, 734, 848 (1949)

(4 constants). Heath & Linnett have also considered an orbital valency force field plus central forces between non-bonded atoms (3 constants) with even greater success. They also applied both of the preceding models to SF_6, SeF_6 and TeF_6 but the results were not as good, particularly for the lowest frequency bending mode[13].

---

13. D. F. Heath and J. W. Linnett, Trans. Far. Soc. 45, 264 (1949).

These models probably fix the force constants fairly adequately but because of the uncertainty it is important that the moments and derivatives be calculated not only for the values derived from the models but for adjacent values, so that the sensitivity to the potential function can be taken into account in arriving at conclusions. We have done this.

a. Tetrahedral Molecules, XY_4

We have used the following symmetry coordinates:

$$R_{1x} = \frac{1}{\sqrt{6}} (\Delta r_1 + \Delta r_2 - 2\Delta r_3),$$

$$R_{2x} = \frac{r_o}{\sqrt{12}}(-2\Delta\alpha_{12} + \Delta\alpha_{23} + \Delta\alpha_{13} - \Delta\alpha_{14} - \Delta\alpha_{24} + 2\Delta\alpha_{34}),$$

$$R_{1y} = \frac{1}{\sqrt{2}}(\Delta r_2 - \Delta r_1)$$

$$R_{2y} = \frac{r_o}{2}(-\Delta\alpha_{23} + \Delta\alpha_{13} + \Delta\alpha_{14} - \Delta\alpha_{24})$$

$$R_{1z} = \frac{1}{\sqrt{12}}(3\Delta r_4 - \Delta r_1 - \Delta r_2 - \Delta r_3)$$

$$R_{2z} = \frac{r_o}{\sqrt{6}}(-\Delta\alpha_{14} - \Delta\alpha_{24} - \Delta\alpha_{34} + \Delta\alpha_{12} + \Delta\alpha_{23} + \Delta\alpha_{13}),$$

where the r's and α's are the bond lengths and angles of Fig. 1, and r_o is the X-Y distance. These coordinates are all chosen so that the direction of motion of the Y atoms is in the positive x, y, or z direction when R is positive.

If it is <u>assumed</u> that stretching produces a change in moment along the bond direction and that bending produces a moment perpendicular to the bond, it is readily shown from the geometry of Fig. 1 that

$$\frac{\partial \mu}{\partial r} = \frac{\sqrt{3}}{2} \quad \frac{\partial \mu}{\partial R_1 \; x(y \text{ or } z)}$$

and

$$\mu_o = \frac{r_o\sqrt{3}}{2} \quad \frac{\partial \mu}{\partial R_2 \; x(y \text{ or } z)} \qquad (25)$$

These equations are most easily obtained from R_{1z} and R_{2z}. The positive sense of all moments is taken from X to Y.

In the calculations $G_{11} = \mu_y + \frac{4}{3}\mu_x$, $G_{12} = \frac{8}{3}\mu_x$ and $G_{22} = 2\mu_y + \frac{16}{3}\mu_x$, where the μ_x and μ_y are the reciprocals of the masses

of atoms X and Y respectively.[9, 12]

b. Octahedral Molecules, XY_6

A convenient set of symmetry coordinates is

$$R_{1x} = \frac{1}{\sqrt{2}}(\Delta r_1 - \Delta r_4),$$

$$R_{2x} = \frac{r_o}{\sqrt{8}}(\Delta\alpha_{46} + \Delta\alpha_{34} + \Delta\alpha_{45} + \Delta\alpha_{24} - \Delta\alpha_{12} - \Delta\alpha_{15} - \Delta\alpha_{13} - \Delta\alpha_{16}),$$

$$R_{1y} = \frac{1}{\sqrt{2}}(\Delta r_3 - \Delta r_6$$

$$R_{2y} = \frac{r_o}{\sqrt{8}}(\Delta\alpha_{56} + \Delta\alpha_{26} + \Delta\alpha_{46} + \Delta\alpha_{16} - \Delta\alpha_{23} - \Delta\alpha_{35} - \Delta\alpha_{34} - \Delta\alpha_{13})$$

$$R_{1z} = \frac{1}{\sqrt{2}}(\Delta r_2 - \Delta r_5)$$

$$R_{2z} = \frac{r_o}{\sqrt{8}}(\Delta\alpha_{15} + \Delta\alpha_{35} + \Delta\alpha_{45} + \Delta\alpha_{56} - \Delta\alpha_{12} - \Delta\alpha_{23} - \Delta\alpha_{24} - \Delta\alpha_{26})$$

where the same conventions are used as before. (See Fig. 2)

In this case

$$G_{11} = 2\mu_x + \mu_y,\ G_{12} = 4\mu_x,\ G_{22} = 8\mu_x + 2\mu_y.$$

The equations utilizing these matrix elements are consistent with those of Eucken and Sauter[14],

---

14. A. Eucken and F. Sauter, Z. fur Phys. Chem. 26B, 453 (1934)

---

and Heath & Linnett[13], but do not agree with those of Wilson, quoted by Yost, Steffens and Gross[15],

---

15. D. M. Yost, C. Steffens, and S. T. Gross, J. Chem. Phys. 2, 313 (1934).

---

which appear to be in error. It should be noted in comparing Linnett's

force constants (f) with ours that

$$F_{11} = f_{11};\ F_{12} = \frac{-f_{12}}{\sqrt{2}},\ F_{22} = \frac{f_{22}}{2}\ .$$

Assuming again that stretching moments are developed along bonds and bending moments perpendicular to them, the geometry of Fig. 2 shows that

$$\frac{\partial \mu}{\partial r} = \frac{1}{\sqrt{2}} \frac{\partial \mu}{\partial R_{1x\,(y \text{ or } z)}} \qquad (26)$$

$$\mu_0 = \frac{r_0}{\sqrt{2}} \frac{\partial \mu}{\partial R_{2x\,(y \text{ or } z)}}$$

Aside from the potential constants, another problem lies in the ambiguity of signs, both of the $\partial\mu/\partial Q$'s obtained from equation (20) and of the coefficients of L^{-1} from equation (23). These ambiguities reflect the indeterminacy in the positive direction of μ with respect to Q, and of Q with respect to Cartesian axes fixed in the molecule. When they are all taken into account, equation (21) yields four solutions but only two different results for the absolute values of $\partial\mu/\partial Rk$. One or the other value is obtained depending on the sign of the ratio $(\partial\mu/\partial Q_1)/(\partial\mu/\partial Q_2)$; the sign ambiguity in L^{-1} merely interchanges the four results. Since there is no loss of generality in doing so, we have chosen the sign of the L^{-1} elements so that each Q has the same sign as the predominant symmetry coordinate in that motion.

It seems worth pointing out that as a consequence of equation (2 an unambiguous value for the ratio $(\partial\mu/\partial R_1)/(\partial\mu/\partial R_2)$ can be found corresponding to each choice of the sign of $(\partial\mu/\partial Q_1)/(\partial\mu/\partial Q_2)$. This has the important consequence that if one of the coordinates (e.g. R_1) is a stretching coordinate and the other (e.g. R_2) a bending coordinate, the ratio of the bond moment to the bond moment

derivative $\partial\mu/\partial r$ is determinate; i.e., if the absolute sign of one is known from any other arguments, the sign of the other may be found from the intensities. Similarly, if they are both bends the relative direction of the bond moments and if they are both stretches the relative signs of the $\partial\mu/\partial r$'s can be found.*

EXPERIMENTAL

The Wilson-Wells extrapolation technique[16]

---

16. E. B. Wilson, Jr., and A. J. Wells, J. Chem. Phys. 14, 578 (1946)

---

was used to obtain the integrated absorption intensity over a complete vibration-rotation band (equation 1). Wilson and wells showed that the intensity as defined by this equation cannot be measured directly with an ordinary spectrometer, but can be obtained from either of the two experimental quantities

$$B = \frac{1}{pl}\int \ln \frac{T_o}{T}\, d\nu$$

$$C = \frac{1}{pl}\int \frac{T_o - T}{T_o}\, d\nu ,$$

where T_o and T are the measured intensities of incident and trans-

---

*Footnote - These statements are readily generalized. If there are g vibrations in a given symmetry class, there are 2^{g-1} independent solutions for each $|\partial\mu/\partial R_k|$ but to each of these solutions corresponds a determinate value for the ratios $(\partial\mu/\partial R_1):(\partial\mu/\partial R_2):\cdots:(\partial\mu/\partial R_g)$ However it is doubtful whether this can prove useful in the more general case.

---

mitted radiation. Briefly, one measures the integrated apparent absorption intensity for unit pressure (B or C) at a series of values of the equivalent path length, and the limiting value, determined as the equivalent path length approaches zero, is the absolute intensity (As an alternative, the limiting slope of the integrated apparent absorption, Bpl or Cpl, as a function of pl may be determined). Atmospheric absorption is kept to a minimum in the region of the band in order that I_o be constant over the slit width, and a sufficiently high pressure of broadening gas is used that the rotational fine structure is eliminated.

The general procedure used in any given run was to measure the absorption at about five different partial pressures of absorbing gas, maintaining the total pressure approximately constant at 800 millimeters with nitrogen. The pressures used were such that the absorption usually varied roughly (peak value) from 35 percent to 8 percent. The adequacy of 800 millimeters total broadening pressure was confirmed by noting in all cases that if a sample of pure gas sufficient to cause about twenty percent absorption was scanned after successive 200 millimeter increments of nitrogen were added, the area of the band had stopped increasing by the time the total pressure was 800 millimeters.

The very low partial pressures required were obtained by successive dilutions of the pure gas with nitrogen. In order to insure complete mixing of the gases, the mixing bulb was equipped with a manual stirrer which was used after each dilution. In addition the bulb was always permitted to stand unused for at least twenty-four hours after every dilution.

The spectrometer used throughout this work was essentially identical with one that has been described in detail in the literature[17].

---

17. D. F. Hornig, G. E. Hyde, and W. A. Adcock, J. Opt. Soc. Am. 40, 497 (1950)

Briefly, it consisted of a double beam optical system used with a Perkin-Elmer model 83 monochromator. The instrument gave a continuous recording of the ratio of light intensity transmitted by sample and blank cells. The instrument had an automatic slit control which maintained the energy received by the detector from the blank path constant.

In all cases "absorption areas" (C) were used as determined directly from the bands obtained on the recorder chart. The area of each band was measured at least twice with a compensating polar planimeter. It was possible to use the areas directly as recorded because the change in dispersion across the bands was small. (In the case of the 632 cm^{-1} CF_4 band and the 615 cm^{-1} SF_6 band it was necessary to divide the bands in halves and treat each half separately to insure that the change in dispersion across these bands would not cause appreciable errors). Since the absorption area is independent of the resolving power[18],

---

18. D. M. Dennison, Phys. Rev. 31, 503 (1928)

---

fairly wide slits were used to obtain a low noise level.

Both the limiting value of C and the limiting slope of C'($\equiv$ Cpl) were determined for each band. The former is shown in figures 3a-8a,

the latter in figures 3b-8b. In addition, the limiting slope of C' was obtained by plotting each individual run separately. These individual runs may be distinguished by the variously shaded circles although the individual C' curves are not shown. The final intensity reported for each band is an average of the following three quantities: (1) the limiting value of C, (2) the limiting slope of C', (3) the average of the limiting slopes of C' obtained from the individual runs. The intensities and $\partial\mu/\partial Q$'s obtained are summarized in Table

A correction for stray light was always made before extrapolation to zero equivalent path length. Only in the case of the 391 cm^{-1} band of SiF_4(KRS-5 region) was the amount of stray light ever greater than 10 percent ($\sim$ 11%).

A consideration of the errors involved in measuring the intensity of absorption shows that the combined errors in the measurement of C probably do not exceed 5 percent. The uncertainty introduced by the extrapolations is estimated to be no greater than 5 percent. Hence the absolute intensities reported should be accurate to $\pm$ 10 percent or better.

SILICON TETRAFLUORIDE

The SiF_4 used was prepared by heating pure barium fluosilicate. The gas formed was passed through a dry-ice-acetone bath to remove non-volatile impurities. It was then condensed in a vacuum system with liquid nitrogen and any non-condensable gases present were pumped off. The SiF_4 thus prepared was thought to be almost 100 percent pure.

A thallium bromide-iodide (KRS-5) prism was used for the 391 cm^{-1}

band. By using a potassium bromide scattering filter and replacing the glass mirror before the entrance slit with one of polished stainless steel, the stray light was reduced to about 11 percent. Since there are atmospheric water bands in this region of the spectrum, the optical path was thoroughly dried. No band was scanned unless the presence of water vapor was indetectable when the spectrometer was operated as a single beam instrument. The average resolution was very roughly estimated to have been 20 to 25 cm^{-1}. The approximate peak to peak noise level on the records was 1 to 1.5 percent.

A rock salt prism was used for the 1031 cm^{-1} band, and the average resolution was about 16 cm^{-1}. The peak to peak noise level on the records was about half a percent.

The results obtained are plotted in Figs. 5a, 5b, 6a and 6b. μ_o, $\frac{\partial \mu}{\partial r}$ and the values of the coefficients of L^{-1} in the equations $Q = L^{-1} R$, are plotted as a function of the potential constants obtained from the general solution over a wide range of values in figure 9. Tho frequencies used in these calculations are listed in Table 2, and the Si-F distance was taken as 1.54 Å[19].

19. L. O. Brockway, Rev. Mod. Phys. 8, 231 (1936)

As mentioned before, the relative signs of μ_o and $\partial\mu/\partial r$ are correct but the absolute signs are indeterminate. The value given by the Simanouti model[12] for F_{11} is indicated by the dashed line and it does not seem likely that the true potential constant differs by more than a few percent from this result. Consequently we can

conclude either that

$$\mu_o = 3.3 \text{ d} \qquad \partial\mu/\partial r = 3.66 \text{ d/A}$$

or

$$\mu_o = 2.3 \text{ d} \qquad \partial\mu/\partial r = -7.49 \text{ d/A}$$

CARBON TETRAFLUORIDE

The CF_4 used was obtained from the Minnesota Mining and Manufacturing Company. It contained about 5 percent fluoroform and traces of carbon dioxide, hexafluoroethane, and an unidentified material. The gas was fractionally distilled twice and it was estimated from the decrease in peak value of the most intense CF_3H fundamental (1152 cm^{-1}) that about 90 percent of the CF_3H originally present was removed. Hence the CF_4 used was of greater than 99 percent purity.

The intensity of the 632 cm^{-1} band was determined using a potassium bromide prism. This band was sufficiently close to the 15 micron carbon dioxide band that it was necessary to exclude atmospheric carbon dioxide. No band was scanned until the strong Q branch of the carbon dioxide fundamental was indetectable on single beam operation. The average resolution used was about 14 to 15 cm^{-1}. A rock salt prism was used for the 1267 cm^{-1} band, and the resolution was roughly 20 cm^{-1}. The peak to peak noise level on the records was less than 1.5 percent in both cases.

The experimental results are plotted in Figs. 7a, 7b, 8a and 8b; μ_o, $\partial\mu/\partial r$ and L^{-1} elements as functions of the potential constants appear in figure 10 in the same way as for SiF_4. The frequencies used in the calculation are listed in Table 2; and 1.36 A was used for the C-F distance[19]. Subsequent to the completion of the calculation a newer investigation[20]

20. P. J. H. Woltz and A. H. Nielsen, J. Chem. Phys. 20 307 (1952)

has assigned ν_3 to a frequency of 1283 cm^{-1}, a change of slightly more than one percent which would not significantly alter the results.

As before, the potential constants of Simanouti lead to the alternate results

$$\mu_o = 2.36\ d \qquad \frac{\partial \mu}{\partial r} = 3.35\ d/A$$

or

$$\mu_o = 1.12\ d \qquad \frac{\partial \mu}{\partial r} = 4.88\ d/A$$

SULFUR HEXAFLUORIDE

The SF_6 used was obtained from the Matheson Company. The only appreciable impurity reported by them was two percent of non-condensable gases (as air) by volume. This was removed by pumping on the condensed gas so that essentially 100 percent pure SF_6 was employed.

A potassium bromide prism was used for the 615 cm^{-1} band and a rock salt prism for the 947 cm^{-1} band. The average resolution was about 11 to 12 cm^{-1} and the peak to peak noise on the records was less than 1.5 percent in both cases.

The results are plotted in Figs. 3a, 3b, 4a and 4b and in Figure 11 as in the previous cases. The frequencies used in the calculations are listed in Table 2. The S-F distance was taken to be 1.57 A^{19}.

The most probable values in Figure 11 are indicated by dashed lines. Although the Heath and Linnett solution does not fit the

lowest bending frequency, $\upsilon(F_2)$, very well (4% error), the constant F_{11} is determined only by the two strong Raman active modes, $\upsilon_{(A1g)}$ and $\upsilon_{(Eg)}$, so we have chosen to determine F_{11} in this way. It is also possible to establish an independent upper limit for F_{11} as follows. Employing the Wilson F and G matrices and using symmetry coordinates to factor the secular determinant[9] yields the following results, where a complete quadratic potential function has been used for the A_{1g} species,

$$A + 4B + L = \lambda(A_{1g})m_y = 6.723 \times 10^5 \text{ dynes/cm;} \qquad (27)$$

for the Eg species,

$$A - 2B + L = \lambda(Eg)m_y = 4.642 \times 10^5 \text{ dynes/cm.} \qquad (28)$$

The definitions of the force constants used are as follows where the notation of Decius[21]

---

21. J. C. Decius, J. Chem. Phys. 16, 1025 (1948)

---

has been employed:

$A \equiv f^2_{rr}$, $B \equiv f^1_{rr}$ (right angles), $L \equiv f^1_{rr}$ (linear). From the above equations it follows that $A + L = 5.336 \times 10^5$ dynes/cm. L is the bond stretching interaction force constant between two bonds lying along a straight line. This constant would be expected to be positive either on the basis of resonance arguments or by considering that there are repulsion forces acting between the F atoms. That is, one would expect the one S-F bond length to decrease if the other S-F bond were stretched. This is further confirmed by the fact that B (the bond stretching interaction force constant for bonds at right angles) is $+ 0.347 \times 10^5$ dynes/cm (obtained from equations (27) and (28). Consequently, if it is assumed that L cannot be less than zero.

then F_{11} cannot be greater than 5.336×10^5 dynes/cm.

Therefore, the most probable results are

$$\mu_o = 0.65 \text{ d} \qquad \text{or} \qquad \mu_o = 2.65 \text{ d}$$

$$\frac{\partial \mu}{\partial r} = -6.58 \text{ d/A} \qquad \frac{\partial \mu}{\partial r} = 3.85 \text{ d/A}$$

CONCLUSIONS

The problem of distinguishing between the alternative solutions is a difficult one, except for SF_6. One would expect a value of approximately 2.2d for the Si-F moment on the basis of electronegativities[22].

---

22. L. Pauling, Nature of the Chemical Bond, Cornell University Press (1948), p. 64 ff.

On the other hand, the dipole moment of SiH_3F has been accurately determined from the microwave spectrum as 1.27d[23].

---

23. A. H. Sharbaugh, V. G. Thomas, and B. S. Pritchard, Phys. Rev. 78, 64 (1950)

This implies either a lower Si-F moment or an Si-H moment of the order of 1d ($\bar{H} - \overset{+}{Si}$). However, both arguments lead to the choice $\mu_o = 2.3$ d and it seems that the error does not exceed $\pm$ 0.3 d.

The difficulty with this conclusion is that the corresponding value of $\partial\mu/\partial r$, -7.5^d/A, is much larger than in the other two molecules as well as of opposite sign; i.e. the moment decreases when the bond is stretched whereas in CF_4 and SF_6 it increases. Consequently, some caution is advisable, particularly since our right to identify μ_o with the static moment of the bond is open to question.

For CF_4, electronegativities suggest a value of roughly 1.5d for the C-F moment[22], intermediate between the two possibilities. The dipole moment of CF_3H is reported to be 1.59d[24]

---

24. K. L. Ramaswamy, Proc. Indian Acad. Sci. 2A, 364 (1935)

---

and this leads to C-F moments of 1.19d or 1.99d, depending on the polarity of the C-H dipole which we assume has a magnitude of 0.4 d.

If the conventional polarity, $\bar{C} - \overset{+}{H}$, is correct, we conclude that we must choose $\mu_0 = 1.12$ d and $\partial\mu/\partial r = 4.9$d/A. However, there are strong theoretical arguments[25, 26]

---

25. C. A. Coulson, Trans. Far. Soc. 38, 433 (1942)

26. W. L. G. Gent, Quart. Rev. 2, 383 (1948)

---

for the polarity $\overset{+}{C} - \bar{H}$, and in this case the other choice, 2.36d, becomes the better. Moreover, if the true value of F_{11} is 5.6×10^5 dynes/cm. rather than 5.2×10^5 dynes/cm., the moment corresponding to positive $(\partial\mu/\partial Q_1)/(\partial\mu/\partial Q_2)$ would be reduced to 2.0 d. Consequently, a clear choice on this basis seems impossible at present.

In a study of CH_3F, Barrow and McKean[27]

---

27. G. M. Barrow and D. C. McKean, Proc. Roy. Soc. (London) A213, 27 (1952)

---

found $\partial\mu/\partial r = 4.70$d/A for the C-F bond (the less reasonable alternative was 4.50d/A), a value close to that associated with the lower dipole moment.

Therefore it seems most likely that $\partial\mu/\partial r = 4.88d/A$. The magnitude of the moment increases as the bond is stretched (this last conclusion is valid in either case). We must also conclude then that in CF_3H the polarity is $\overset{-}{C} - \overset{+}{H}$.

The choice is a little easier for SF_6. An electronegativity based on di- or tetravalent sulfur (s-p hybridization[22]) predicts an S-F moment of about 1.5d but in hexacovalent sulfur (s-p-d hybridization) the moment might be expected to be greater. It seems reasonable that the hexavalent S-F moment should be greater than that of Si-F. Since one of the choices is only 0.65d, it seems quite likely that $\mu_0 = 2.65$ d is correct, in which case $\partial\mu/\partial r = 3.85d/A$ and the moment increases as the bond stretches. The only reservation that must be made is that if F_{11} is actually as great as 6×10^5 dynes/cm., the other choice of ratio also leads to a sufficiently large μ_0. However since, as was pointed out before, this would require a large negative stretch-stretch interaction term in the potential function, it seems safe to discount the possibility.

The most striking feature of the results for all three molecules is the large value obtained for $\partial\mu/\partial r$. Except in CH_3F such large values have been obtained previously only for highly resonant molecules such as CO, N_2O, CO_2 and COS. The fact that the moment in CF_4 and SF_6 increases as the bond is stretched implies that if F is at the negative end of the dipole at equilibrium the negative ion resonance form becomes more pronounced as the bond is stretched, in good agreement with the usual resonance argument. However, if our earlier conclusions are correct the magnitude of $\partial\mu/\partial r$ is even greater in SiF_4 than in CF_4 or SF_6 and the moment decreases when

the bond is stretched. For this we have no present explanation although one can formally include a no-bond resonance form to produce this result. Nevertheless, this would still not explain the great difference between SiF_4 and the other two. The fact that the value of $\partial\mu/\partial r$ obtained for the C-F bond in CF_4 is so nearly the same as in CH_3F where there cannot be much resonance implies that the large values may be associated with bonds to fluorine rather than resonance in the molecules.

Finally, the sensitivity of our results to the choice of potential function leads us to conclude that no bond moment or derivative calculated from the infrared intensities of a polyatomic molecule can be regarded as reliable unless the general potential function has been determined accurately or the sensitivity of the result to reasonable variations in the potential function has been calculated.

TABLE 1

Absolute Intensities (cm^{-1}/cm atm) And $\frac{\partial \mu}{\partial Q}$ Values (e.s.u.)

For SiF_4, CF_4 and SF_6.

SiF_4	CF_4	SF_6
A (ν_3) ----- 2635 (Q_1)	A (ν_3) ---- 4540 (Q_1)	A (ν_5) --- 4800(Q_1)
A (ν_4) ----- 507 (Q_2)	A (ν_4) ---- 41.7 (Q_2)	A (ν_6) --- 280(Q_2)
$\frac{\partial \mu}{\partial Q_1}$ ----- $\pm$167.4	$\frac{\partial \mu}{\partial Q_1}$ ---- $\pm$219.8	$\frac{\partial \mu}{\partial Q_1}$ --- $\pm$226.1
$\frac{\partial \mu}{\partial Q_2}$ ----- $\pm$ 73.45	$\frac{\partial \mu}{\partial Q_2}$ ---- $\pm$21.07	$\frac{\partial \mu}{\partial Q_2}$ --- $\pm$54.62

TABLE 2

Fundamental Frequencies of SiF_4, CF_4 and SF_6 (cm^{-1})

SiF_4[28]	CF_4	SF_6
$\nu_1(A1)$(liq.)=800	$\nu_1(A_1)$ =904[29]	$\nu_1(A_{1g})$ =775[31]
$\nu_2(E)$ (liq.)=268	$\nu_2(E)$(liq.)=437[29]	$\nu_2(E_g)$(liq.)=644[31]
$\nu_3(F_2)$ =1031(Q_1)	$\nu_3(F_2)$ =1267(Q_1)[30]	$\nu_3(F_{2g})$(liq.)=524[31]
$\nu_4(F_2)$ = 391(Q_2)	$\nu_4(F_2)$ =632.5(Q_2)[30]	$\nu_4(F_{2u})$ =363[31]
		$\nu_5(F_{1u})$ =947(Q_1)[32]
		$\nu_6(F_{1u})$ =615(Q_2)[31]

28. E. A. Jones, J. S. Kirby-Smith, P. J. H. Woltz, and A. H. Nielsen J. Chem. Phys. 19, 242 (1951).

29. D. M. Yost, E. N. Lassetre, and S. F. Gross, J. Chem. Phys. 4, 325 (1936).

30. J. R. Nielsen, C. M. Richards, and H. L. McMurry, J. Chem. Phys. 16, 67 (1948).

31. R. T. Lagemann and E. A. Jones, J. Chem. Phys. 19, 534 (1951).

32. D. Edelson and K. B. McAfee, J. Chem. Phys. 19, 1311 (1951).

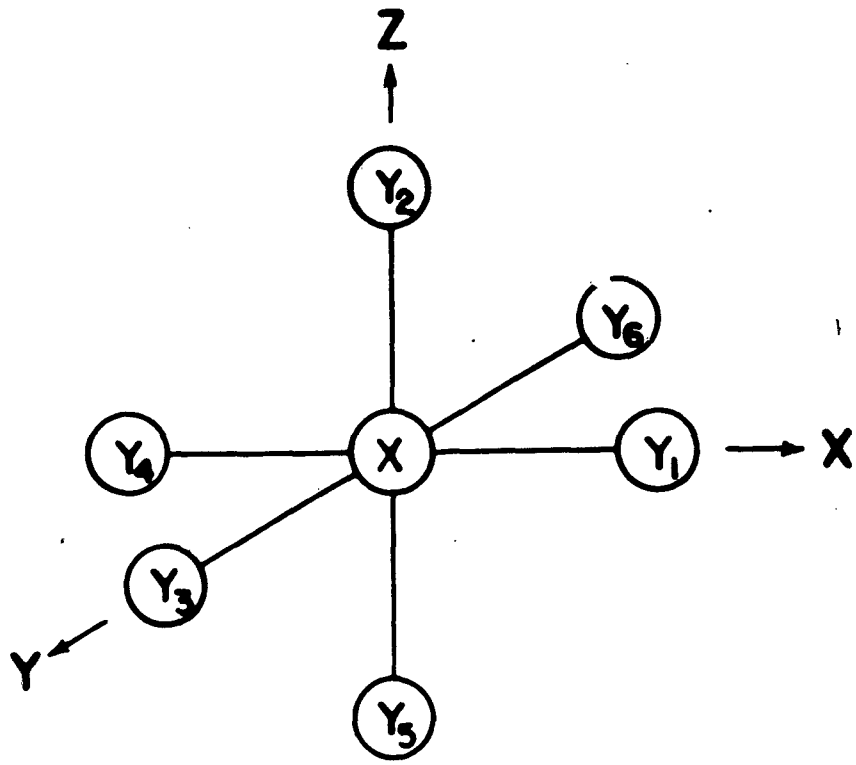

FIG. 2

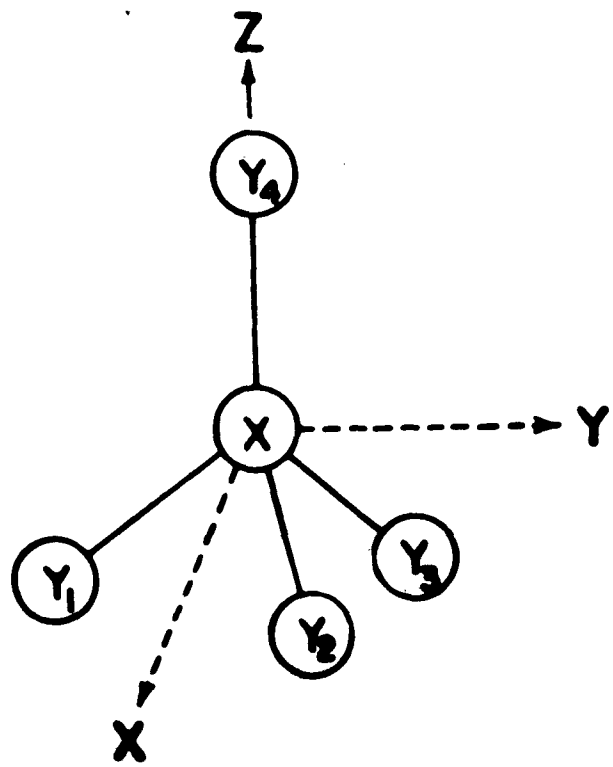

FIG. 1

EXPERIMENTAL INTENSITY DATA FOR THE 615 Cm^{-1} BAND OF SF_6

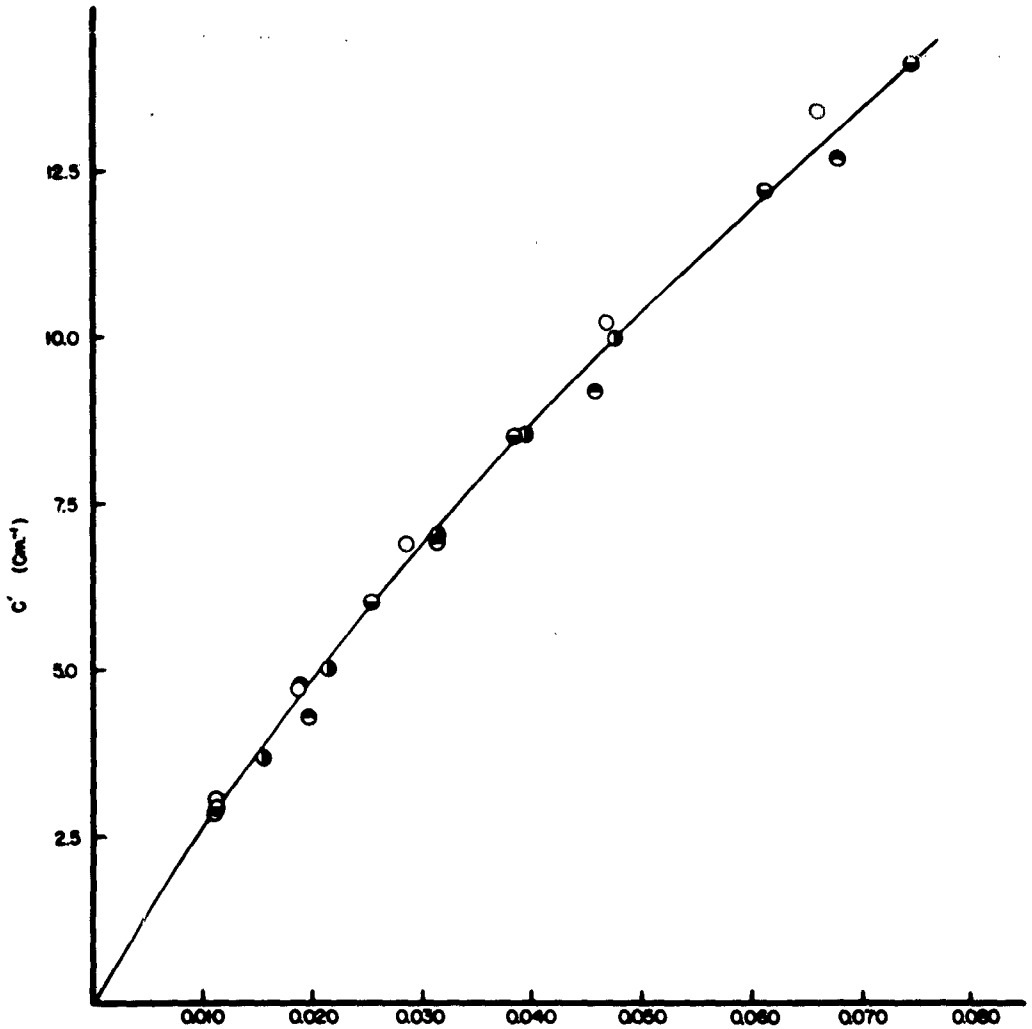

FIG. 3a

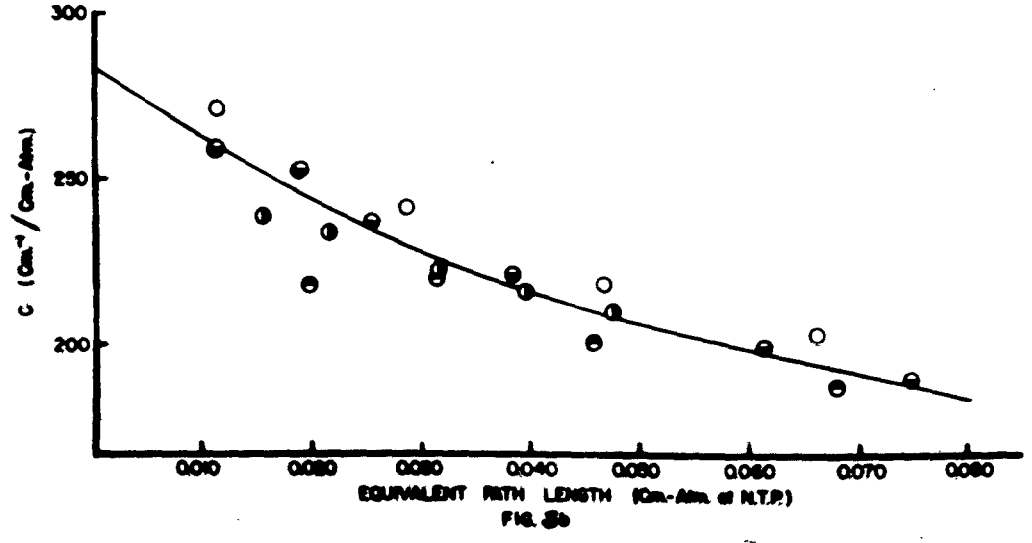

FIG. 3b

EXPERIMENTAL INTENSITY DATA FOR THE 947 $Cm.^{-1}$ BAND OF SF_6

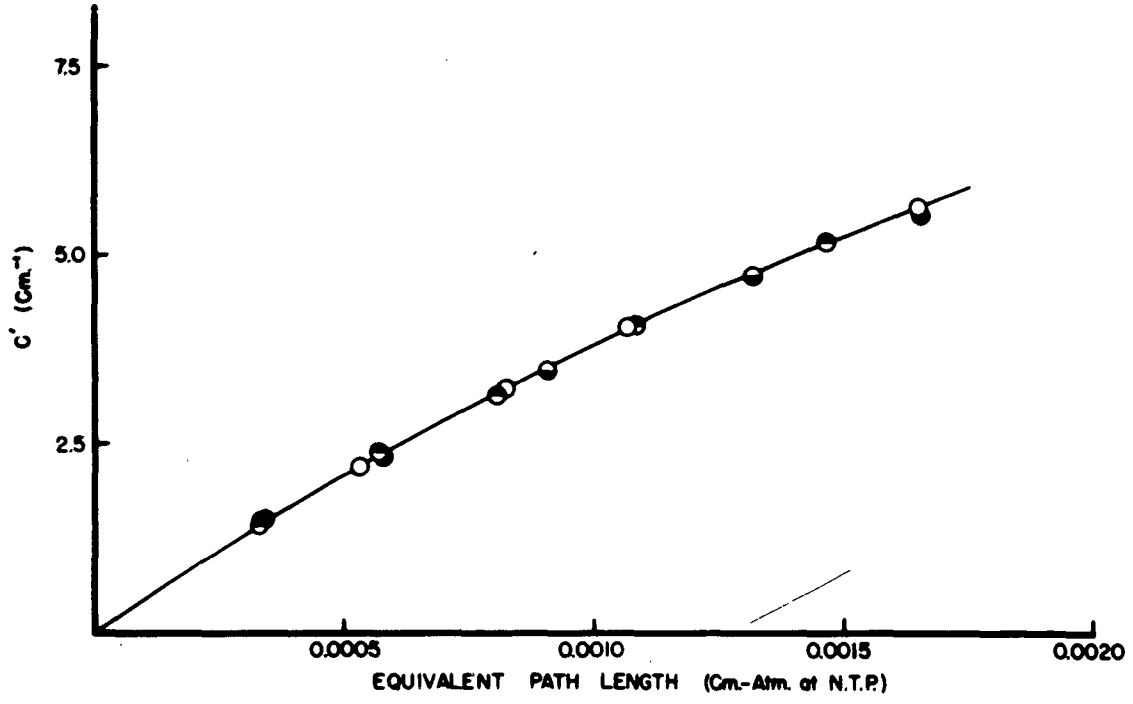

FIG. 4a

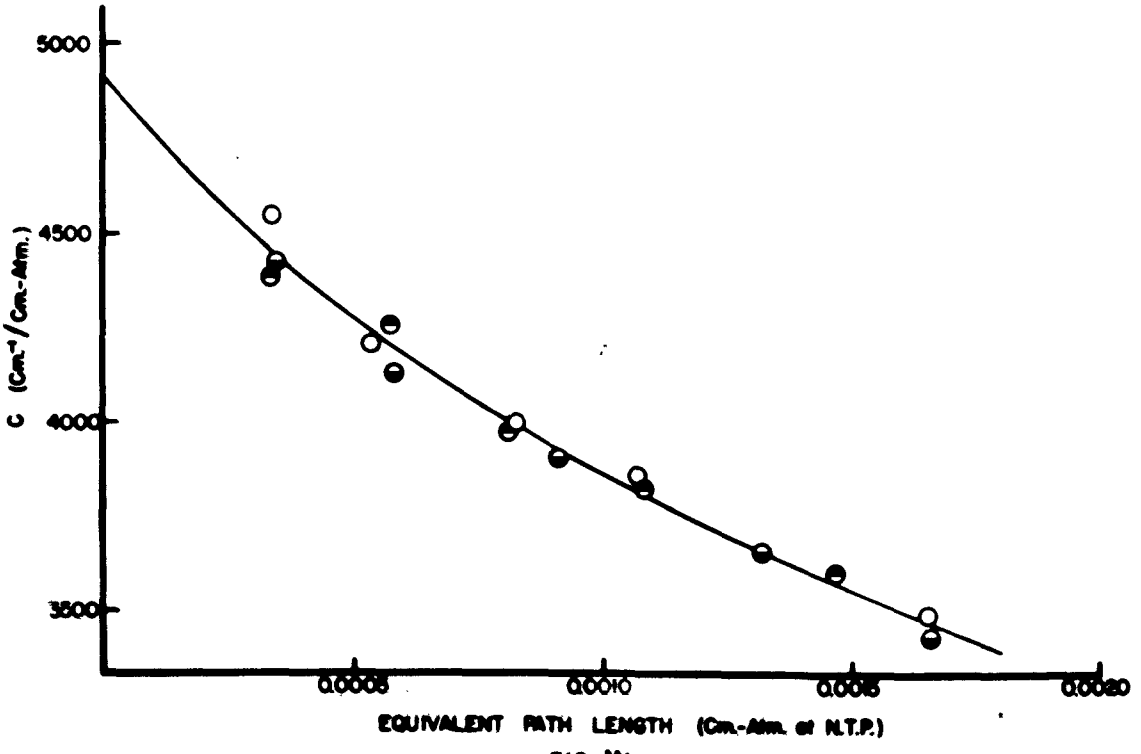

FIG. 4b

EXPERIMENTAL INTENSITY DATA FOR THE 391 Cm^{-1} BAND OF SiF_4

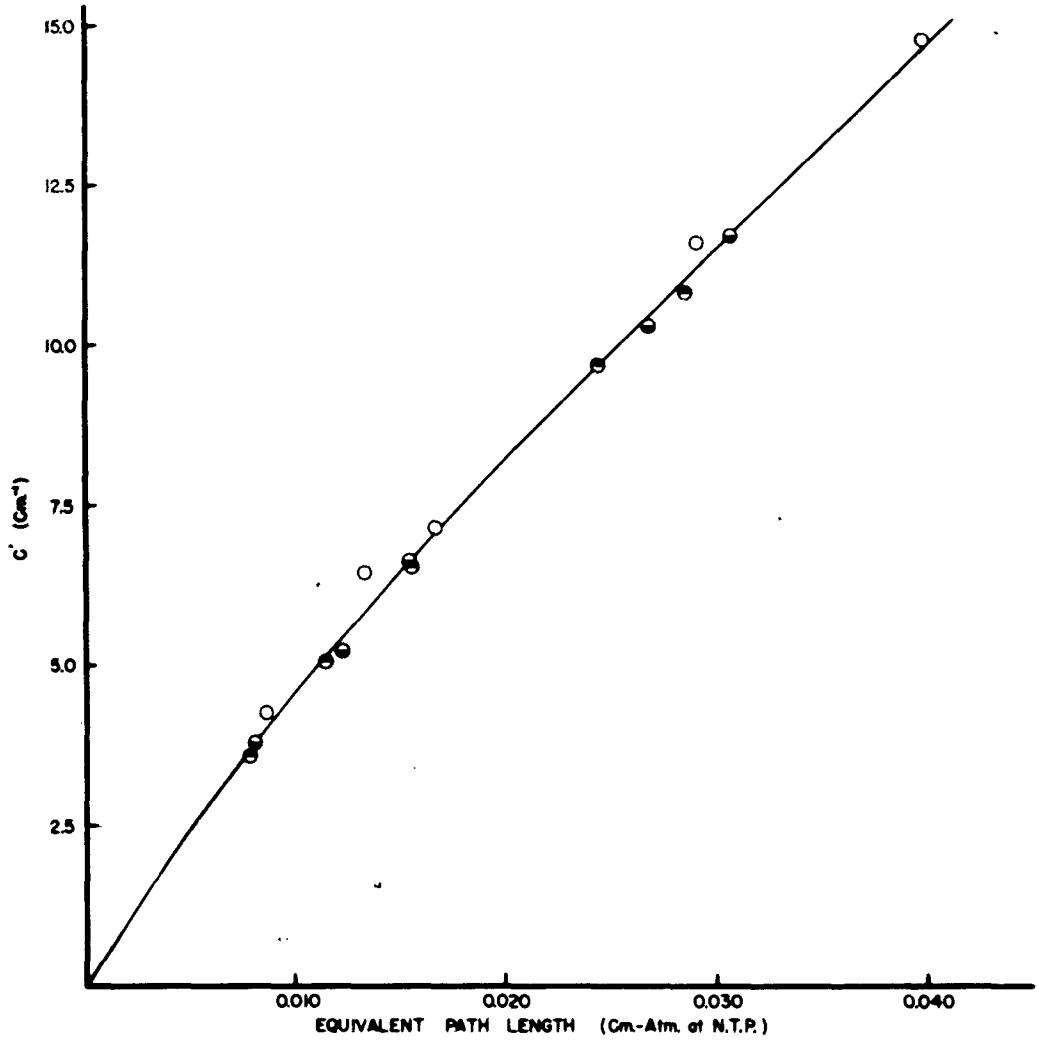

FIG. 5a

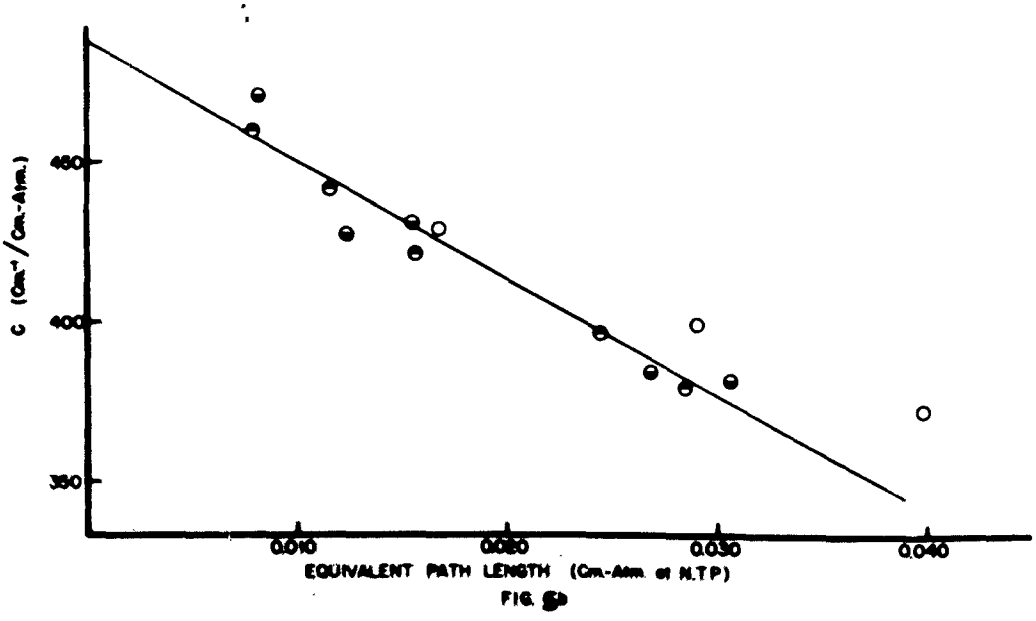

FIG. 5b

EXPERIMENTAL INTENSITY DATA FOR THE 1031 Cm^{-1} BAND OF SiF_4

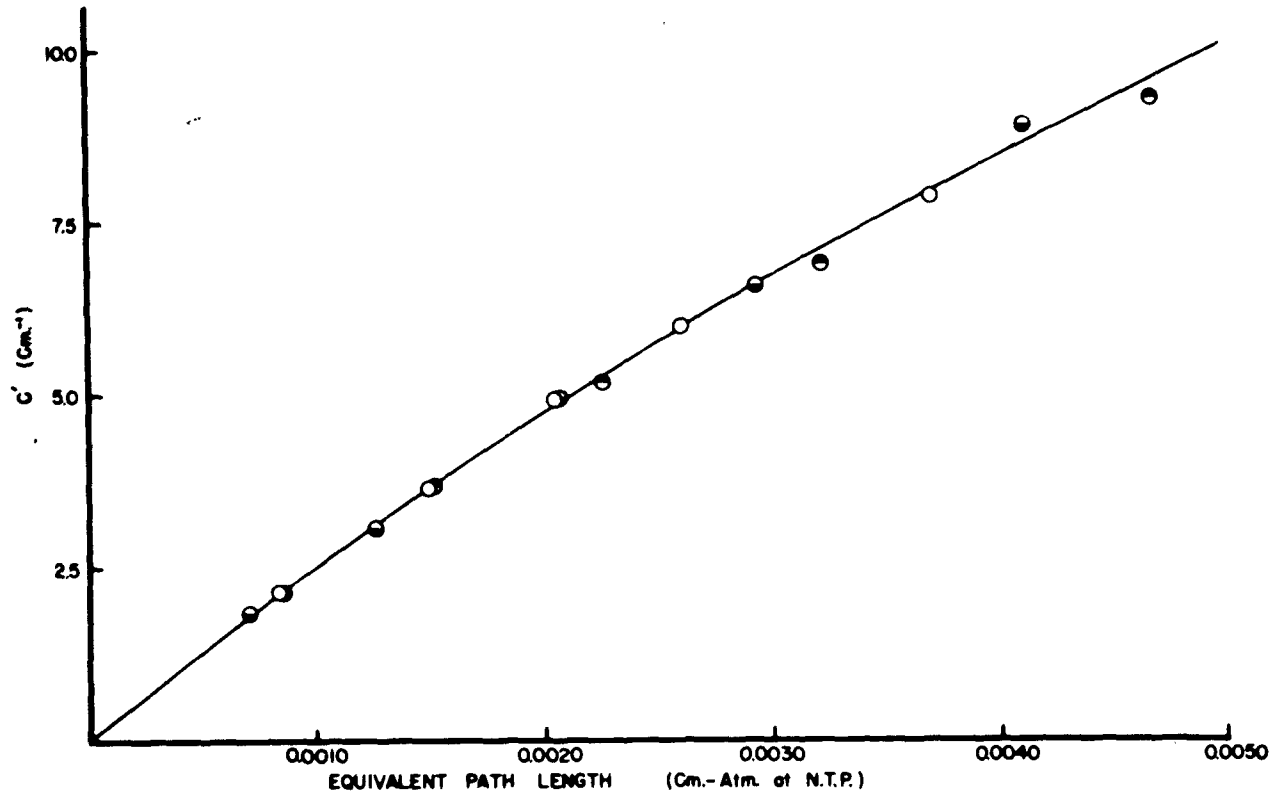

FIG. 6a

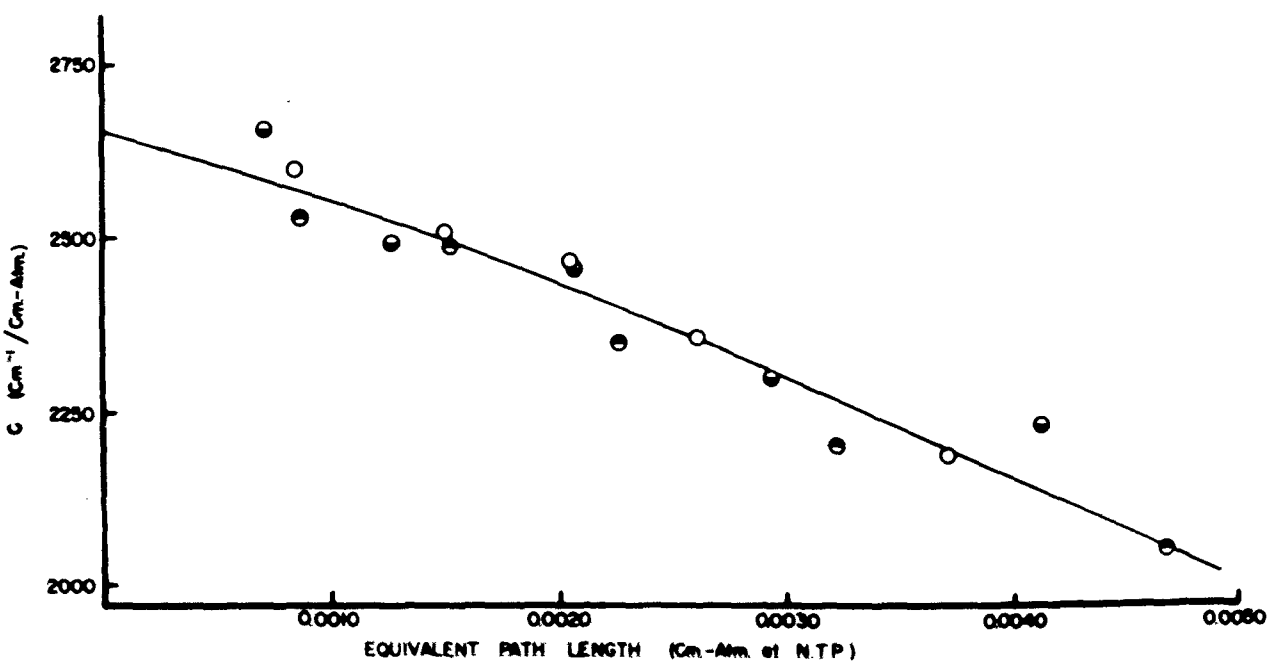

FIG. 6b

EXPERIMENTAL INTENSITY DATA FOR THE 632 $Cm.^{-1}$ BAND OF CF_4

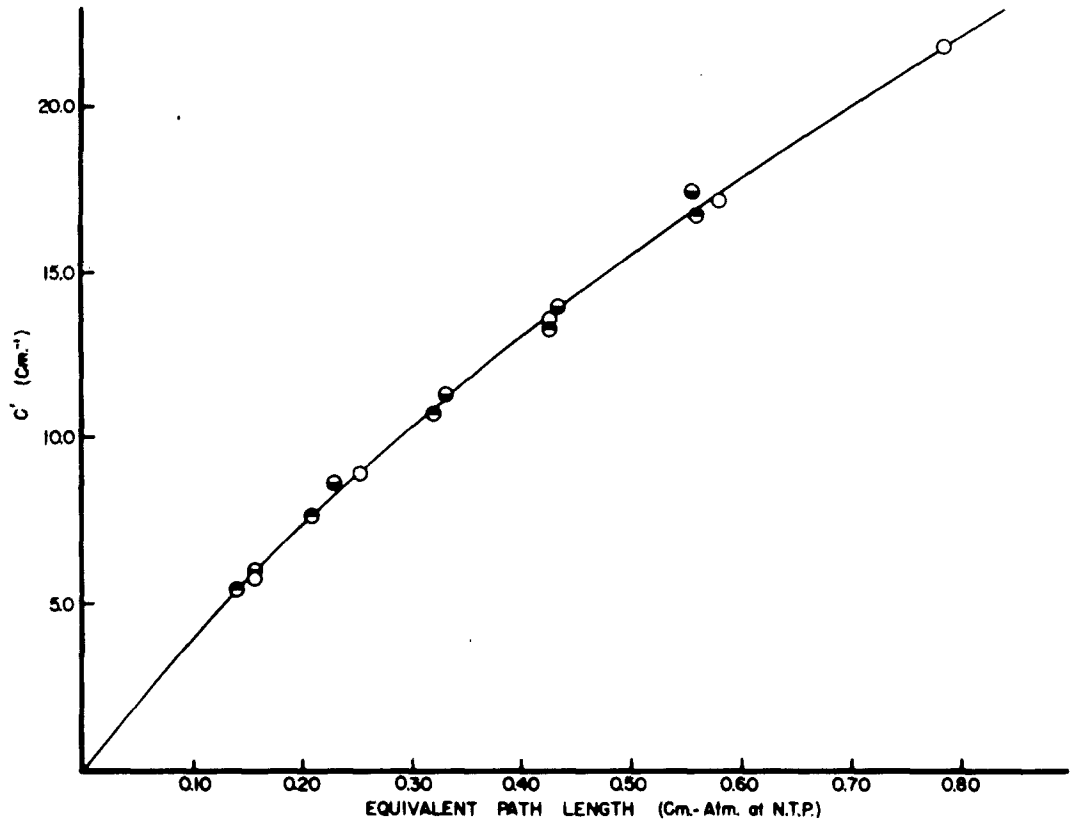

FIG. 7a

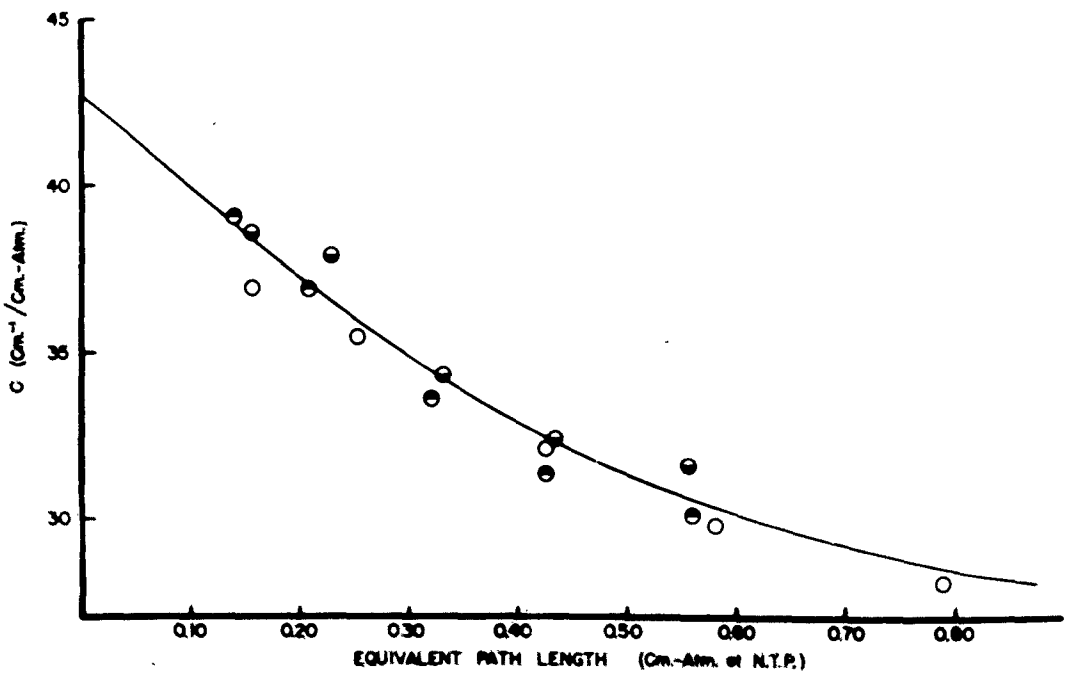

FIG. 7b

51

EXPERIMENTAL INTENSITY DATA FOR THE 1267 $Cm.^{-1}$ BAND OF CF_4

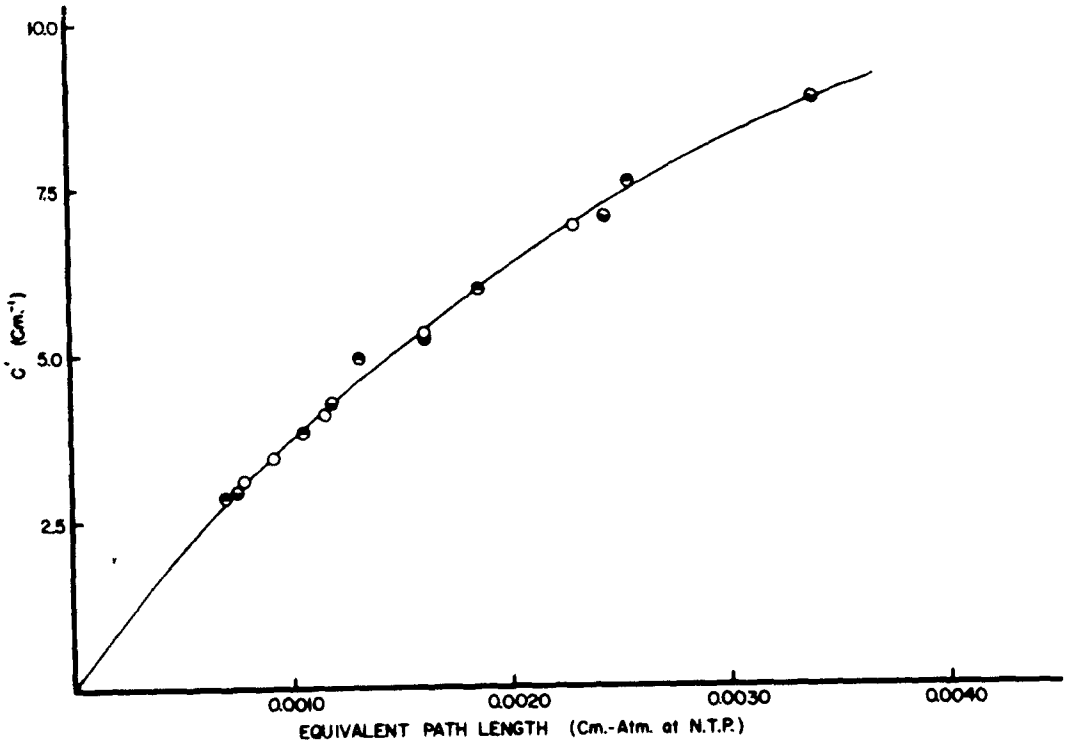

FIG. 8a

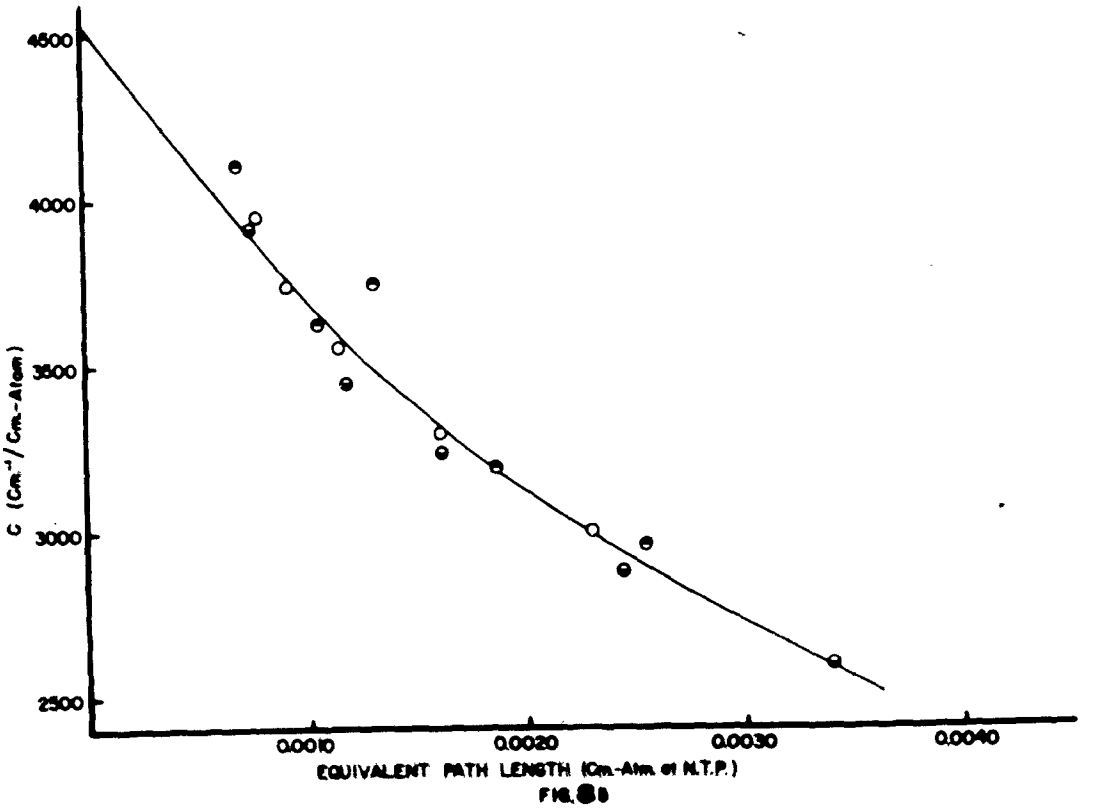

FIG. 8b

FIGURE 9 - SiF_4

(A) Bond Moments (d) and Bond Moment Derivatives (d/A);

(B) Coefficients in Normal Coordinates (x 10^{12});

(C) Force Constants (x 10^{-5});

as functions of the Si-F stretching force constant, F_{11} (x 10^{-5}). Dashed line indicates most probable value of F_{11}.

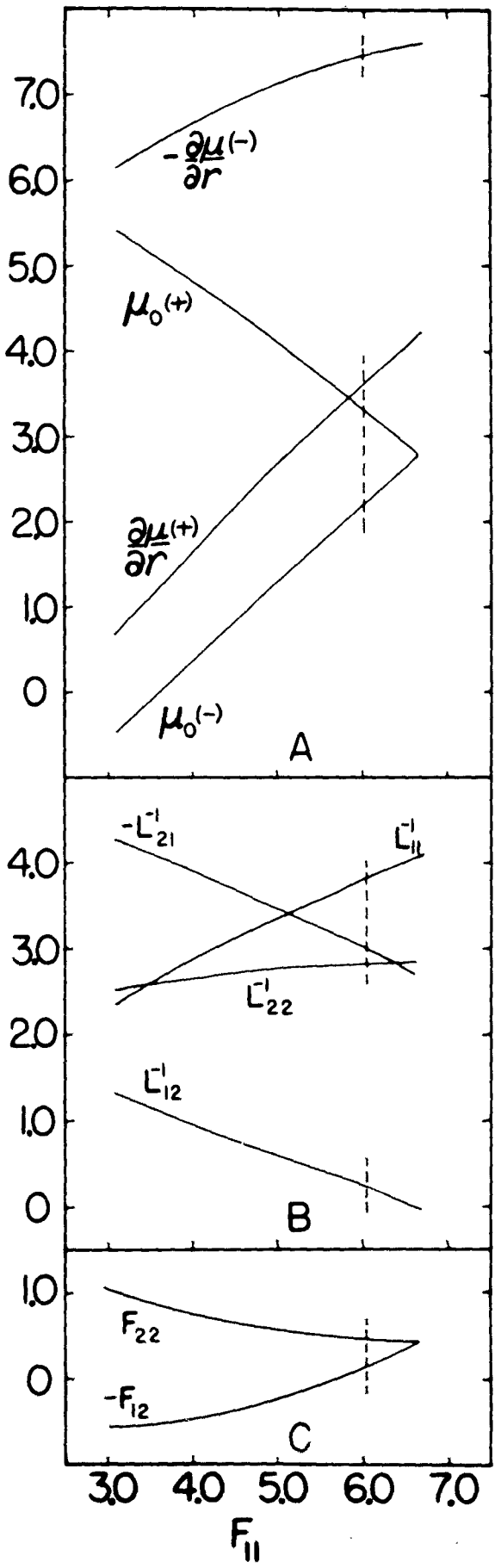
7.0
6.0
5.0
4.0
3.0
2.0
1.0
0
$-\frac{\partial \mu^{(-)}}{\partial r}$
$\mu_0^{(+)}$
$\frac{\partial \mu^{(+)}}{\partial r}$
$\mu_0^{(-)}$
A
$-L^{-1}_{21}$
L^{-1}_{11}
L^{-1}_{22}
L^{-1}_{12}
B
F_{22}
$-F_{12}$
C
3.0
4.0
5.0
6.0
7.0
F_{11}

FIG 9
S: F_4

FIGURE 10 - CF_4

(A) Bond Moments (d) and Bond Moment Derivatives (d/A);

(B) Coefficients in Normal Coordinates ($\times 10^{12}$);

(C) Force Constants ($\times 10^{-5}$);

as functions of the C-F stretching force constant, F_{11} ($\times 10^{-5}$). Dashed line indicates most probable value of F_{11}.

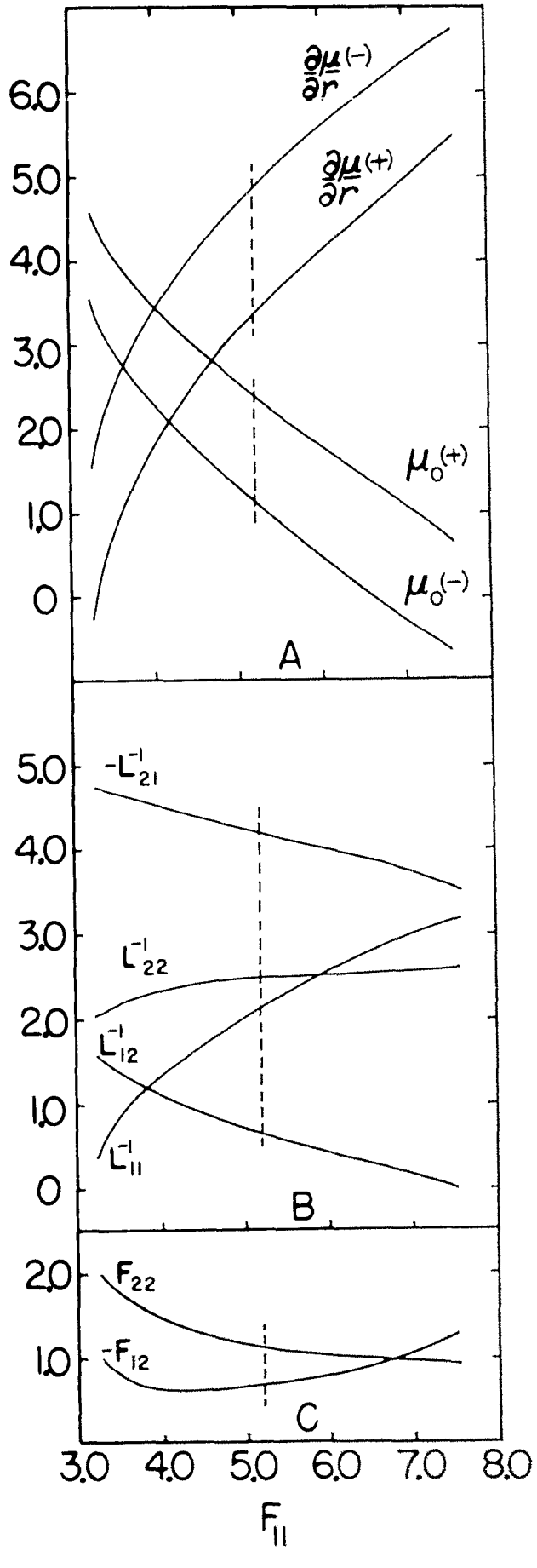
6.0
5.0
4.0
3.0
2.0
1.0
0
$\frac{\partial \mu}{\partial r}^{(-)}$
$\frac{\partial \mu}{\partial r}^{(+)}$
$\mu_0^{(+)}$
$\mu_0^{(-)}$
A
5.0
4.0
3.0
2.0
1.0
0
$-L_{21}^{-1}$
L_{22}^{-1}
L_{12}^{-1}
L_{11}^{-1}
B
2.0
1.0
F_{22}
$-F_{12}$
C
3.0
4.0
5.0
6.0
7.0
8.0
F_{11}

FIG. 10
CF_4

FIGURE 11 - SF_6

(A) Bond Moments (d) and Bond Moment Derivatives (d/A);

(B) Coefficients in Normal Coordinates ($\times 10^{12}$);

(C) Force Constants ($\times 10^{-5}$);

as functions of the S-F stretching force constant, F_{11} ($\times 10^{-5}$). Dashed line indicates most probable value of F_{11}.

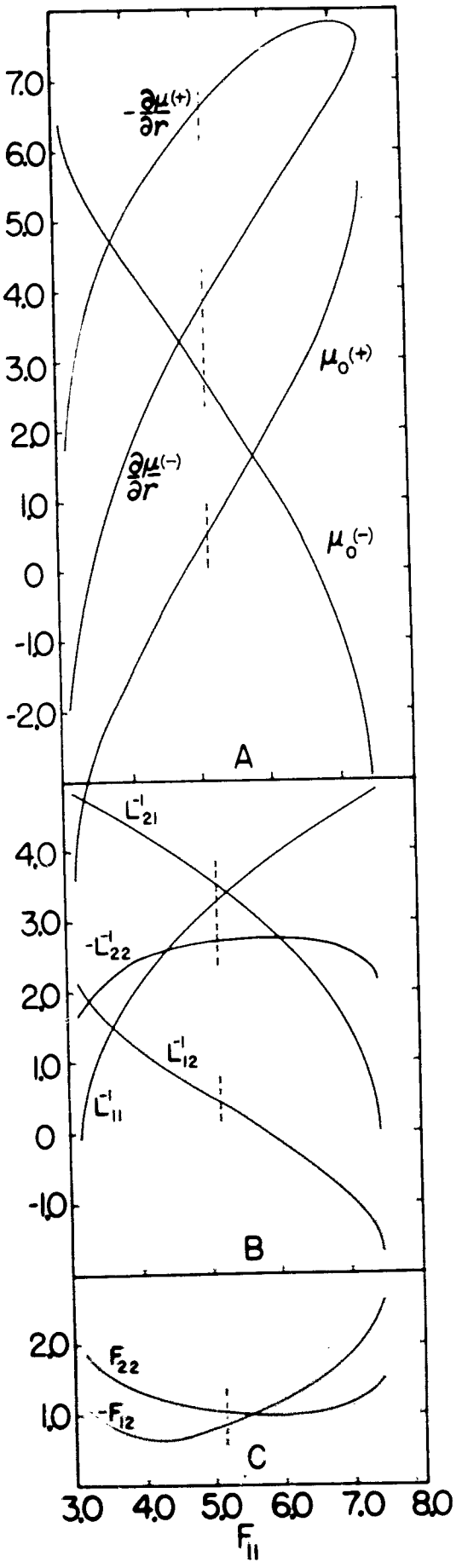
7.0
6.0
5.0
4.0
3.0
2.0
1.0
0
-1.0
-2.0
$-\frac{\partial \mu^{(+)}}{\partial r}$
$\mu_0^{(+)}$
$\frac{\partial \mu^{(-)}}{\partial r}$
$\mu_0^{(-)}$
A
L^{-1}_{21}
4.0
3.0
$-L^{-1}_{22}$
2.0
L^{-1}_{12}
1.0
L^{-1}_{11}
0
-1.0
B
2.0
F_{22}
1.0
$-F_{12}$
C
3.0
4.0
5.0
6.0
7.0
8.0
F_{11}

FIG. 11
SF_6

Reprinted from JOURNAL OF THE OPTICAL SOCIETY OF AMERICA, Vol. 42, No. 10, 774–778, October, 1952
Printed in U. S. A.

The Design of Photoelectric Raman Apparatus*

WILLIAM R. BUSING†
Metcalf Chemical Laboratories, Brown University, Providence, Rhode Island

(Received June 19, 1952)

The performance of a photoelectric Raman spectrograph depends on the amount of luminant energy transmitted to the photomultiplier. An expression for this energy is found and this leads directly to certain principles to be followed in the design of such an instrument. The optimum sample shape is discussed and various types of sources are compared.

PERHAPS the greatest single advance in experimental Raman spectroscopy since its discovery in 1928 has been the introduction in recent years of photoelectric methods for the detection and recording of the spectrum.[1] The primary advantage which is gained by the elimination of the photographic process is a response curve which is linear and free from the inherent irreproducibility of the older technique. For this reason a photoelectric instrument should provide better intensity measurements, more reliable polarization data, and more accurate information on band shapes. Furthermore, the convenience of an instrument which presents the data in immediately usable form is a factor which cannot be overlooked.

On the other hand, because a photoelectric instrument must scan the spectrum, it necessarily makes less efficient use of the scattered light than does a photographic spectrograph which can record all wavelengths simultaneously. Moreover, the effective exposure time, i.e., the response time of the electronic circuits, is limited in practice to less than a minute. These limitations make it necessary to use considerable care in designing a spectrograph for photoelectric use. In this paper we shall discuss the various factors involved in the design of such an instrument.

GENERAL

A good photoelectric Raman spectrograph should be capable of providing satisfactory resolution together with a high signal to noise ratio. In many cases it is desirable to obtain this result with a limited amount of sample.

The signal to noise ratio of a photoelectric detector depends largely on the amount of luminant energy which it receives.[2] The reason for this is that if the photocurrent is much less than the dark current, the noise will be substantially constant and the signal to noise ratio will be proportional to the light intensity. For strong light signals the noise increases as the square root of the photocurrent so that an increase in intensity will still improve the signal to noise ratio.

Figure 1 shows schematically the optics of a typical photoelectric Raman spectrograph. Included is the sample which is irradiated by the exciting light, the condensing lens, the entrance and exit slits, the collimating and camera lenses or mirrors, and the dispersing elements. In Appendix I it is shown that the total energy transmitted by the system is given by:

$$E = kilh_1 a\nu^2 ld/f_1. \tag{1}$$

Here k is a constant, i is the average intensity of the excitation in watts/cm^2, l is the length of the sample, h_1 is the height of the entrance slit, a is the area of the limiting aperture, ν is the spectral slit width in cm^{-1}, d is the dispersion in radians cm^{-1}, t is the efficiency of the optical system, and f_1 is the focal length of the collimator.[3]

The energy transmitted depends on the square of the spectral slit width, and, since the resolving limit imposed by diffraction can seldom be reached with the intensities available in Raman spectroscopy, this spectral slit width is usually a direct measure of the resolution.‡ As long as this condition is satisfied it will always be possible to increase the signal to noise ratio of a given instrument by sacrificing resolution and vice versa. In practice it is necessary to choose a suitable compromise between these factors. It is evident that any change in the design of an instrument which tends to increase the energy transmission will also tend to improve the resolution.

MONOCHROMATOR

It is therefore desirable to provide the monochromator with slits as high as practical. The optics should have a large effective area, and the focal length of the collimator must be as short as possible. The prisms or grating should be efficient and have a high dispersion. There is little preference between the two types of dispersing elements, however, because, although gratings often have the higher dispersion, prisms are usually more efficient.§

* This work was supported by the ONR.
† Present address: Sterling Chemistry Laboratory, Yale University, New Haven, Connecticut.
[1] Rank, Pfister, and Coleman, J. Opt. Soc. Am. 32, 390 (1942). D. H. Rank and R. Wiegand, J. Opt. Soc. Am. 36, 326 (1946).
[2] R. W. Engstrom, J. Opt. Soc. Am. 37, 420 (1947).
[3] Similar expressions have been derived by Perry (Proc. Phys. Soc. (London) 50, 265 (1938)) in order to compare monochromators used for irradiation purposes and by Strong (Phys. Today 4, No. 4, 14(1951)) in discussing the design of an infrared spectrograph.
‡ The resolving limit of a single dense flint glass prism 10 cm on a side is about 1 cm^{-1} at 4358A.
§ This is in contrast with the design requirements of a photographic instrument which responds to energy *density* rather than

For comparing various monochromators quantitatively it may be desirable to use the figure of merit, h_1adl/f_1, obtained by factoring the pertinent parameters from (1). For example, it may be shown that the grating monochromator of Rank and Wiegand[1] has approximately the same figure of merit as the Perkin-Elmer Model 83 prism monochromator. The shorter focal length of the latter instrument compensates for the higher dispersion and larger aperture of the former. An instrument which has been constructed in this laboratory[4] with longer slits, large prisms, and a relatively short focal length has a figure of merit two to three times larger than that of either of the above monochromators. No exact figures are given because good estimates of l are unavailable for some of these instruments.

SAMPLE

It has been assumed in the previous discussion that the sample is high enough and wide enough to embrace the entire optical path of the spectrograph. It is well known that under these conditions the position and focal length of the condensing lens or the distance of the sample from the entrance slit can have no effect on the energy transmission but that the latter depends only on the sample length, l.[5] The dimensions of the sample required do depend on these factors, however, and also on the design of the monochromator in a way which has been treated by Poole.[6] Using his results we obtain an expression for the volume of a sample with rectangular cross section:

$$V=(\beta h_1 m/2\mu\alpha)[1/m+l/2\mu f_c(1+m)]+\beta m^2/4\mu^2\alpha^2 \quad (2)$$

where f_c is the focal length of the condensing lens, m is the magnification of the image of the sample on the entrance slit, α is the ratio of the collimator focal length to the diameter of the limiting aperture, and μ is the refractive index of the sample.

If it is necessary to reduce the sample volume the two parameters which have an appreciable effect on V and which are readily adjustable are l and h_1. It is clear from (1) that a decrease in l will have the same effect on the energy as a proportional decrease in h_1. From (2), however, it is apparent that a decrease in l will have a much greater effect on the sample volume than a proportional decrease in h_1. With a given volume of sample the best performance can be obtained by using the entire entrance slit and making the cell as short as necessary.‖

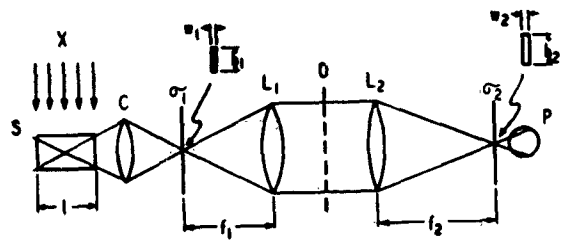

FIG. 1. The optical system of a typical photoelectric Raman spectrograph showing the sample, S, which is irradiated by the exciting light, X, the condensing lens, C, the entrance and exit slits, σ_1 and σ_2, the collimating and camera lenses (or mirrors), L_1 and L_2, the prisms or grating, D, and the photomultiplier, P.

SOURCE

Finally it is necessary to design the source so that the excitation intensity, i, is as large as possible. This not only means that the lamps must operate at high power but also that the radiation must be efficiently concentrated on the sample. Because of the wide variety of sources in general use it was decided to make some simple calculations to compare various designs and to gain an understanding of the factors influencing their intensities. For this purpose the *geometrical efficiency*, g, of a source will be defined as the fraction of the total light of the lamps which would fall on a Raman sample presenting an area of one cm² in every direction. It will be assumed that this total light is proportional to p, the power consumed by the lamps, so that the intensity at the sample is given by:

$$i \propto gp.$$

gp may then be used as a figure of merit for estimating the relative performance of a source.

In Appendix II approximate expressions for g are derived for six types of sources. These are listed in Table I together with numerical values of gp for some representative designs. A few remarks may be made about each type of source on the basis of these calculations.

A simple source, consisting of lamps at a distance r from the sample (or a single spiral arc surrounding it), has a low efficiency but high powered lamps may be used. Since the efficiency is proportional to $1/r^2$ it may be more desirable to use a small number of lamps close to the sample than a larger number at a greater distance. The results show that the addition of a single circular cylindrical reflector does not increase the intensity of a simple source substantially.

to total energy. It is shown in Appendix I that this energy density is given by:

$$I=kll_2da/f_1^2$$

where f_1 is the focal length of the camera lens. In this case the performance depends on neither the dispersion nor the slit height and it is the camera lens rather than the collimator which must have a short focal length. Furthermore, because high dispersion is no longer important, a prism instrument with its high efficiency probably has the advantage over a grating instrument for photographic work.

[4] W. R. Busing and D. F. Hornig, *Symposium on Molecular Structure and Spectroscopy* (Ohio State University, June, 1951).

[5] J. R. Nielsen, J. Opt. Soc. Am. 28, 701 (1938).

[6] H. G. Poole, J. Chem. Soc. 1946, 245.

‖ For example, a sample 5 cm long used with a slit 2 cm high produces the same energy as a sample 10 cm long used with a 1 cm slit, but using typical values for the parameters ($m=1$, $\mu=1.5$, $\alpha=5.0$, $f_c=30$ cm) we calculate that the former has a volume of 4.0 cc while the volume of the latter is 11.5 cc.

This conclusion applies only to photoelectric instruments. A decrease in h_1 has little effect on the performance of a photographic spectrograph so that with the latter instrument the entrance slit should be masked and a long narrow cell should be used.

TABLE I. The efficiencies and relative intensities of various Raman sources. (See Appendix II for derivations.)

Type of source	Efficiency, g	Meaning of symbols	Representative source of each type: Typical values	Relative intensity, gp, in watts/cm²
Simple source	$1/4\pi r^2$	r —distance of lamps from sample p —total lamp power	8 cm 2000 watts	2.5
Simple source with circular cylindrical reflector	$(1/4\pi)[1/r^2+1/(2b-r)^2]$	r —distance of lamps from sample b —radius of reflector p —total lamp power	8 cm 11 cm 2000 watts	3.2
Elliptical reflectors (See Fig. 2)	$1/4\pi r^2+m/2bnd$	r —distance of lamps from sample b —major axis of ellipse d —diameter of lamps n —number of lamps m—metallic reflection coefficient p —total lamp power	8 cm 11 cm 2.5 cm 2 0.9 500 watts	4.8
			Same source with $n=4$, $p=1000$ watts	5.5
Spherical lens	$b^2/4v^2hd$	b —radius of lens v —image distance h —length of lamp d —diameter of lamp p —total lamp power	8 cm 30 cm 15 cm 2.5 cm 500 watts	0.24
Cylindrical lens	$b/4\pi v(u+v)d$	b —width of lens v —image distance u —object distance d —diameter of lamp p —total lamp power	10 cm 30 cm 30 cm 2.5 cm 500 watts	0.09
Enclosed diffuse reflector (MgO)	$(c/b^2)\beta/(1-\beta)+1/4\pi r^2$	c —empirical constant r —distance of lamps from sample b —radius of reflector β —average reflection coefficient p —total lamp power	0.04 8 cm 11 cm 0.85 500 watts	1.6
			Same source with $p=2000$ watts	6.2

Sources using elliptical reflectors have a high efficiency, and in practice they should compare favorably with simple sources of higher power. The calculations show that it is again desirable to keep the lamps close to the sample and that the major axis of the ellipse must be made as small as possible.

Unfortunately there are certain limitations on the power which can be used efficiently in such a source. High powered lamps with suitable spectral characteristics for Raman work usually must be large in diameter. The calculations show, however, that a large lamp diameter results in a low efficiency. For this reason, and also because large lamps will generally require larger values of r and b, increasing the power of the individual lamps may provide only a limited improvement in the intensity.

Furthermore, the number of lamps cannot be increased without eliminating the most effective part of each ellipse (See Fig. 2 (c)). Using the expression for g we find that if p' is the power of each lamp and there are n lamps then

$$gp = p'm/2bd + p'n/4\pi r^2.$$

Since the first term is usually large compared to the second, the number of lamps has only a small effect on the intensity. This is illustrated by the two sources of this type which are described in Table I. It will be seen that in this case doubling the number of lamps adds only about 15 percent to the intensity.

It is evident from the calculations that sources using either spherical or cylindrical lenses are usually much less intense than any of the other types considered here. The primary reason for this is that the lens itself can intercept only a small fraction of the total light.

Recently a new type of source has been introduced which uses a completely enclosed diffuse reflector of magnesium oxide.[7] Because the amount of light is effectively multiplied by many reflections this type of source is potentially the most intense known. The contribution of these multiple reflections appears in the expression for the efficiency as the factor $\beta/(1-\beta)$ where β is the *average* reflection coefficient. If β can be kept close to unity the efficiency will be very high. On the other hand, any opening in the reflector which allows light to escape lowers the value of β and therefore decreases the efficiency of the source. If much light

[7] A. C. Menzies and J. Skinner, J. Sci. Instr. 26, 299 (1949).

escapes in this way the advantage of the diffuse reflector is lost.

In practice the requirement that the source be enclosed may cause some inconvenience. It should also be pointed out that small changes in β may cause appreciable changes in the efficiency so that intensity measurements may not be as reproducible as those made with other sources.

Using the general principles which have been set forth here, a photoelectric recording Raman spectrograph has been designed and built in this laboratory. This instrument has already been described briefly,[4] and a more detailed account of its performance is being prepared for publication.

The author wishes to express his appreciation to Professor Donald F. Hornig for suggesting this problem and for his helpful discussions throughout the work.

APPENDIX I

Derivation of the Energy Transmission

The slits of a monochromator will ordinarily be adjusted so that

$$w_1 = w_2 f_1 / f_2, \tag{3}$$

where w_1 and w_2 are the entrance and exit slit widths, respectively, and f_1 and f_2 are the collimating and camera lens focal lengths. The exit slit width is related to the spectral slit width, ν, by the equation:

$$w_2 = \nu d f_2 \tag{4}$$

where d is the dispersion in radians/cm^{-1}.

Because the intensity of a Raman source depends only on the sample length, l, and the exciting intensity, i, we may treat the source as though it were an infinite plane glowing with an intensity proportional to il.[5] E', the energy entering the monochromator, is proportional to the area of the entrance slit, $w_1 h_1$, and also to the solid angle subtended by the optics so that

$$E' = k' i l w_1 h_1 a / f_1^2$$

where a is the area of the limiting aperture and k' is a constant. The fraction of the entering energy which leaves the exit slit is proportional to the spectral slit width and also to l, the efficiency of the optical system. The over-all energy transmission is then given by:

$$E = k i l h_1 \nu d a' / f_1^2. \tag{5}$$

Substituting (3) and (4) in (5) we have

$$E = k i l h_1 a \nu^2 l d / f_1.$$

If the instrument is photographic rather than photoelectric its performance is determined by the energy density instead of the total energy. Dividing (5) by $w_2 h_2 = w_1 h_1 f_2^2 / f_1^2$ we obtain

$$I = E / w_2 h_2 = k i l \nu a / f_1^2.$$

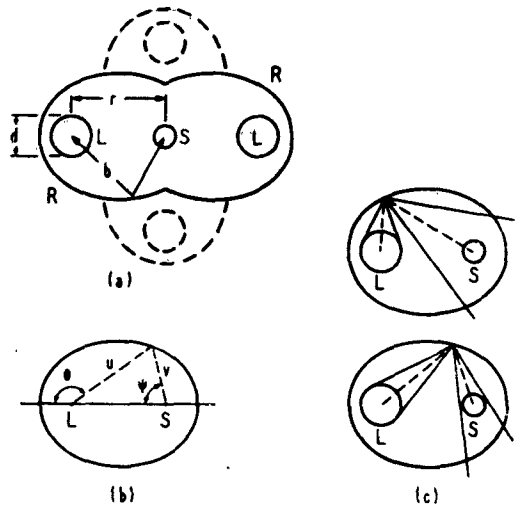

FIG. 2. A Raman source using elliptical reflectors. (a) Top view showing the lamps, L, the sample, S, and the reflectors, R. The dashed lines indicate the possibility of using more than two lamps. (b) Parameters used in the derivation of g for the elliptical reflectors. θ is the angle about the lamp, L, and ψ is the angle about the sample, S. (c) Top view of the ellipse showing how the finite diameter of the lamps decreases the efficiency of the source. Comparison of the two figures shows that portions of the ellipse near the sample are more efficient than those near the lamp.

APPENDIX II

The Efficiency of Various Sources

The geometrical efficiency, g, of a source has been defined as the fraction of the total light which would fall on a test sample presenting an area of one cm^2 in every direction. Approximate expressions for g will now be found for six types of sources.

Simple source.—In this source the sample is irradiated directly by the lamps without the aid of lenses or reflectors. It may be shown that no large error is introduced by assuming that every volume element of the lamps is at approximately the same distance, r, from the sample. If each element radiates uniformly in all directions then the efficiency is given by:

$$g = 1/4\pi r^2.$$

Simple source with circular cylindrical reflector.—The focusing effect of a circular reflector and the contribution of multiple reflections may be shown to be negligible. If the radius of the reflector is b, then this source has the properties of a simple source with a second ring of lamps at a distance of $2b-r$ from the sample and

$$g = (1/4\pi)[1/r^2 + 1/(2b-r)^2].$$

Elliptical reflectors.—The top view of a typical source using elliptical reflectors is shown in Fig. 2(a). To calculate g we shall consider separately light leaving the lamp within each increment of the horizontal angle, θ. (See Fig. 2 (b).) g will then be found by integrating these contributions over θ.

Each ray of light which reaches the sample via the

reflector travels a distance approximately equal to the major axis, b, of the ellipse. The vertical angle (i.e., the angle in a plane perpendicular to the page in Fig. 2) subtended by a test sample one cm square is then $1/b$. The fraction of the light leaving the lamp within this vertical angle and also within the increment of solid angle, $d\theta$, is $d\theta/4\pi b$.

Not all of this light falls on the test sample, however, because of the finite diameter of the lamp and the horizontal magnification effect which is illustrated in Fig. 2(c). The diameter of the lamp image at the sample is $v(\theta)d/u(\theta)$ where u and v are the object and image distances, respectively. The fraction of the image falling on a sample one cm wide is then $u(\theta)/v(\theta)d$. The fraction of the total light which reaches the test sample via an element of the ellipse which subtends an angle $d\theta$ is given by:

$$dg=m(d\theta/4\pi b)[u(\theta)/v(\theta)d]$$

where m is the metallic reflection coefficient. Integrating over θ and adding the effect of light which reaches the sample without reflection we have:

$$g=1/4\pi r^2+(m/4\pi bd)\ 2\int_0^{\psi-\pi/n}[u(\theta)/v(\theta)]d\theta$$

where ψ is the angle about the sample as shown in Fig. 2(b) and n is the number of lamps. r is again the distance of the lamps from the sample.

It may be shown that for any ellipse

$$\int_0^{\psi-\psi'}[u(\theta)/v(\theta)]d\theta=\psi'$$

so that

$$g=1/4\pi r^2+m/2bnd.\P$$

Spherical lens.—In this source an image of the lamp is focused on the sample by an ordinary spherical lens. If the radius of the lens is b and its distance from the lamp is u then the fraction of the total light which falls on the lens is $\pi b^2/4\pi u^2=b^2/4u^2$. This light forms an image of the lamp which has an area v^2hd/u^2 where d and h are the diameter and height of the lamp respectively and v is the image distance. The fraction of the total light falling on the one cm² test sample is then

$$g=(b^2/4u^2)(u^2/v^2hd)=b^2/4v^2hd.\P$$

Cylindrical lens.—In this type of source an image of the lamp is formed on the sample by a cylindrical lens. Since there is no focusing effect in the vertical plane (i.e., the plane containing the axes of the lamp, lens, and sample), a one cm square test sample will subtend an angle of $1/(u+v)$ in this plane where u and v are the image and object distances, respectively. In the horizontal plane (perpendicular to these axes) the lens of width b subtends an angle of b/u. The fraction of the total light emitted within the solid angle defined by these two plane angles is $b/4\pi u(u+v)$. Not all of this light falls on the test sample, however, because of the finite diameter d, of the lamp. The width of the image is vd/u and the useful fraction is u/vd so that the expression for the efficiency is

$$g=[b/4\pi u(u+v)](u/vd)=b/4\pi v(u+v)d.\P$$

Enclosed diffuse reflector.—In this type of source the intensity is effectively multiplied by many reflections within a diffuse reflector which is almost completely enclosed. We shall obtain an expression for g in a semi-empirical manner which does not involve the calculation of the distribution of light flux.

Let β be the average reflection coefficient of the interior of the reflector (including the effect of holes which allow light to escape). On each reflection the incident light is multiplied by the fraction β so that the total reflected light is equal to the original light times $\beta+\beta^2+\beta^3+\cdots=\beta/(1-\beta)$. The reflector is then effectively a lamp with $\beta/(1-\beta)$ times the power of the real lamps. Adding the effect of direct radiation we may write

$$g=(c/b^2)\beta/(1-\beta)+1/4\pi r^2 \qquad (6)$$

where r is the distance of the lamps from the sample, b is the radius of the reflector, and c is a constant to be determined empirically.

A source with $b=7.6$ cm, $r=6.3$ cm, and $\beta=0.86$ (calculated) was tested photoelectrically in this laboratory. By comparing measurements of the intensity of the Raman spectrum of CCl_4 with and without the diffuse reflector the first term of (6) was found to be 2.3 times the second and from this data c was calculated to be 0.044. While it is true that c must depend to some extent on the geometry of the reflector, this figure should be useful for estimating the order of magnitude of g for any source of this type.

¶ It should be noted that in the case of sources using elliptical reflectors or lenses, the expressions for g which are derived here will give intensities which are approximately correct only over the region occupied by the image of the lamp. If the sample is larger than the image the effective intensity of the source will be less than that calculated.

Reprinted from THE JOURNAL OF CHEMICAL PHYSICS, Vol. 20, No. 9, 1345–1347, September, 1952
Printed in U. S. A.

The Vibrational Spectra of Molecules and Complex Ions in Crystals. VI. Carbon Dioxide*

W. E. OSBERG† AND D. F. HORNIG
Metcalf Chemical Laboratories, Brown University, Providence, Rhode Island
(Received April 14, 1952)

A previously reported discrepancy between the predicted and observed infrared spectrum of crystalline carbon dioxide is shown to arise from the presence of two peaks due to $C^{13}O_2$, a combination band involving a lattice frequency near 110 cm^{-1} and two reflection peaks. The infrared spectrum was studied at −190°C and aside from the previous features shows one component from ν_1 and two from ν_3, shifted very little from the gas frequencies. The difficulties encountered in interpreting the spectrum of this simple crystal occur quite generally in the spectra of more complicated substances.

INTRODUCTION

IT has been pointed out that the reported infrared spectrum of crystalline carbon dioxide is incompatible with the structure determined by x-ray diffraction studies.[1] Such a discrepancy in so simple a molecular crystal seemed worthy of further investigation.

According to the x-ray structure determinations, carbon dioxide forms a face-centered cubic lattice of symmetry T_h^6 with four molecules per unit cell.[2–4]

The molecules all lie on sites of symmetry $C_{3i}(\equiv S_6)$. This site symmetry alone is sufficient to establish that the exclusion rule between infrared and Raman spectra should hold, as indeed it does. Only the Fermi doublet arising from the symmetric stretching vibration (ν_1) has been observed in the Raman spectrum,[5] while the antisymmetric stretching vibration (ν_3) and the bending vibration (ν_2) were found only in the infrared spectrum.[6]

The relation between the vibrations of the isolated molecule and of the active vibrations arising from the coupled motions of the molecules in the crystal is just the relation between the site symmetry and the space group.[7]

This relation is illustrated for the present case in Fig. 1. It is seen that ν_1 should give rise to two components in the crystal. They may both be Raman active. In fact this vibration is split by Fermi resonance with $2\nu_2$, just as in the gas, and no further splitting has been observed. The antisymmetric vibration ν_3 should give rise to two components (species A_u and F_u of T_h) of which only the second should be infrared active in the crystal. However, two peaks have been reported by Dahlke.[6] Finally, the bending vibration ν_2 should yield three components in the crystal, one of species E_u and two of species F_u. Only the latter pair should be active, but three peaks were observed. Consequently, we have reinvestigated the infrared spectrum of crystalline carbon dioxide in order to determine the origin of these differences.

EXPERIMENTAL RESULTS

Commercial carbon dioxide‡ whose purity was stated to be 99.5 percent was used for the work. The maximum amounts of impurity were stated to be 0.34 percent nitrogen, 0.09 percent oxygen, and 0.07 percent water vapor. The infrared spectrum of the gas disclosed no impurity which might affect the results of this investigation.

The films were prepared by subliming the CO_2, which had previously been condensed in a cold trap,

* Based on a thesis presented by W. E. Osberg in partial fulfillment of the requirements for the degree of Doctor of Philosophy, Brown University, 1951. This work was supported by the ONR.
† Present address: Hercules Powder Company, Wilmington, Delaware.
[1] D. F. Hornig, Disc. Faraday Soc. No. 9, 115 (1950).
[2] J. de Smedt and W. H. Keesom, Proc. Amsterdam Acad. 27, 839 (1924); Z. Krist. 62, 312 (1926).
[3] H. Mark and E. Pohland, Z. Krist. 61, 293 (1925); 64, 113 (1926).
[4] J. C. McLennan and J. O. Wilhelm, Trans. Roy. Soc. Can. Sec. III (3) 19, 51 (1925).
[5] J. C. McLennan and H. D. Smith, Can. J. Research 7, 551 (1932).
[6] W. Dahlke, Z. Physik 102, 360 (1936).
[7] D. F. Hornig, J. Chem. Phys. 16, 1063 (1948).
‡ Pure Carbonic Company, Boston, Massachusetts.

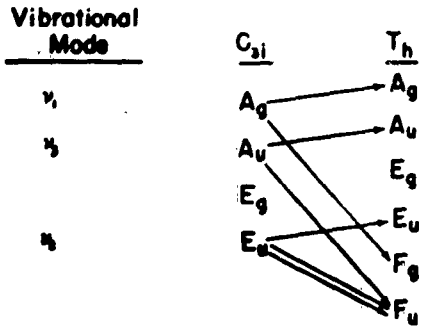

FIG. 1. Relation between the local symmetry of CO_2 in the crystal and the symmetry of the unit cell containing 4 molecules.

onto an NaCl backing plate which was mounted in a low temperature transmission type cell maintained at a temperature of −190°C. The resulting films were quite transparent to the eye, except for the thickest ones, and showed little scattering in the infrared region.

The spectra were obtained at −190°C on a double-beam infrared spectrophotometer,[8] using CaF_2, NaCl, and KBr prisms. They are shown in Figs. 2 to 5 and the results tabulated in Table I. The frequencies given are believed to be accurate to ±5 cm^{-1} at 3700 cm^{-1}, ±3 cm^{-1} at 2350 cm^{-1}, and ±1 cm^{-1} at 650 cm^{-1}. The spectrum of crystalline carbon dioxide obtained in the present work agrees well with that of Dahlke in the vicinity of 650 cm^{-1} and 3600 cm^{-1}. However, it is quite different in the neighborhood of 2300 cm^{-1}, and the absorption maximum which was reported at 2288 cm^{-1} actually occurs at 2344 cm^{-1}. Since the spectrometer was calibrated on the atmospheric carbon dioxide band at 2349 cm^{-1} before and after each run, it does not seem possible that the present results are in error. In addition, the study of a thick film revealed an absorption band at 637 cm^{-1} which had not been reported previously.

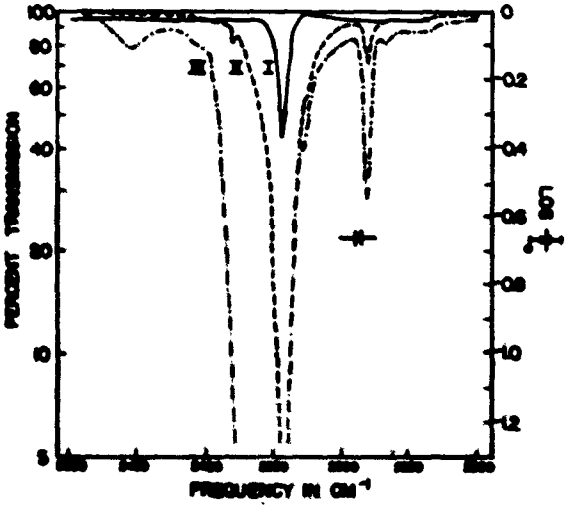

FIG. 2. The infrared spectrum of crystalline CO_2 at −190°C in the region of the fundamental ν_3.

[8] Hornig, Hyde, and Adcock, J. Opt. Soc. Am. 40, 697 (1950).

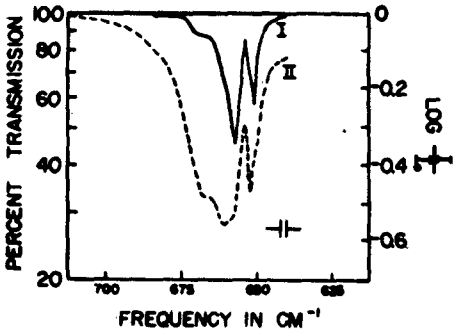

FIG. 3. The infrared spectrum of crystalline CO_2 at −190°C in the region of the fundamental ν_3 taken with NaCl prism.

DISCUSSION

It is to be expected that at this low temperature (−190°C) all of the fundamental vibrations should yield sharp lines in the infrared spectrum.[7] If all of the sharp lines in the spectrum of the thin film are assigned to the fundamentals, the pattern of lines coincides exactly with that expected theoretically. Only one line which can be ascribed to the asymmetric stretching vibration ν_3 is observed (Fig. 2), and in contrast to the earlier work this line has a frequency only 5 cm^{-1} different from that found in the gas. Similarly, two sharp lines due to the bending vibration ν_2 are observed. The mean observed width of these three lines at half the maximum absorption coefficient is only 5 cm^{-1}; most of the width of ν_3 and of the less intense component of ν_2 certainly originates in the finite resolution of the spectrometer, but the more intense component of ν_2 appears to have a natural width of approximately 3 cm^{-1}. Consequently, there appears to be no genuine discrepancy.

In addition to these three lines there are two sharp but weak bands which can be ascribed unambiguously to $C^{13}O_2$. Since the vibration frequencies of the $C^{13}O_2$ molecule differ from those of the surrounding molecules, the $C^{13}O_2$ spectrum should be simple, showing no structure caused by intermolecular coupling. This is indeed the case and only one peak due to ν_2 is found in $C^{13}O_2$ in contrast to $C^{12}O_2$ which shows two. This effect has

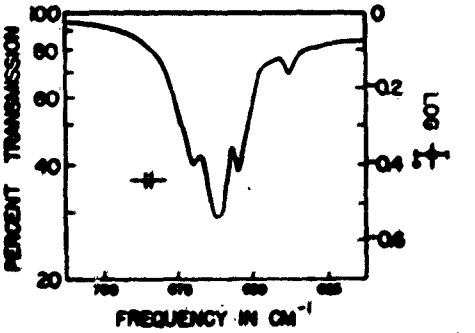

FIG. 4. The infrared spectrum of crystalline CO_2 at −190°C in the region of the fundamental ν_2 taken with a KBr prism.

been observed previously in solid solutions of HCl in DCl[9] and of naphthalene in anthracene.[10]

Aside from the peaks near 3600 cm^{-1} which are readily interpreted in terms of the large number of components of the two combinations lying in this vicinity (all of which may resonate) and those at 667 cm^{-1} and 2379 cm^{-1} which we believe are caused by reflection, all that remains is the relatively broad peak at 2454 cm^{-1} and a region of extremely weak absorption, scarcely above the noise level in the thickest film, between 2235 and 2270 cm^{-1}. It seems highly probable that the former arises from a combination of ν_3 with the torsional oscillation frequencies of the molecules in the lattice with a maximum density of frequencies near 110 cm^{-1}. It is not impossible, however, that the combination involves translational lattice frequencies since the $u-g$ selection rule applies only to limiting modes[11] but the selection rules for limiting modes appear to be valid empirically, no definite violations having yet been found. The absorption near 2260 cm^{-1} may arise from the corresponding difference bands.

TABLE I. Infrared absorption frequencies of crystalline carbon dioxide at −190°C.

Gas (cm^{-1})	Crystal (cm^{-1})	$\Delta\nu$ (cm^{-1})	Line width (cm^{-1})	Assignment
	3748[a]		...	
3716	3712	−4	27	$\nu_1+\nu_3$ and
	3639[a]		...	$2\nu_2+\nu_3$
3609	3610	+1	26	
	2454		35	$\nu_3+\nu$ Torsion
	2379[a]		...	Reflection
2349	2344	−5	7	ν_3
2284	2280	−4	7	ν_3 ($C^{13}O_2$)
	667	...	...	Reflection
	660		7	
667		−10		ν_2
	653		4	
642[b]	637	...	6	ν_2 ($C^{13}O_2$)

[a] Shoulder.
[b] Calculated.

THE EFFECT OF REFLECTION

The effect of reflection from the vacuum-sample and sample-backing interfaces, plus the reflection from the same interfaces traversed in the opposite direction, appear in the spectra of crystals as spurious absorption. Because of the rapid variation of the index of refraction near an absorption band the reflectivity of each interface varies widely in the neighborhood of an absorption band and may shift the apparent peak position or produce a spurious peak nearby, usually on the high frequency side. In a recent investigation of the reflection spectra of the ammonium salts, Bovey found reflection peaks shifted as much as 30 cm^{-1} to the high frequency side of the absorption maximum.[12]

However, they have also been observed shifted to low frequencies.[13]

A very characteristic feature of reflection maxima which frequently is sufficient to identify them is their very great intensity increase when the thickness of thin films is increased. This effect arises because the destructive interference of the beams reflected from the front and back surfaces of a vanishingly thin film changes to constructive interference when the film thickness is $\lambda/4$.

Such behavior is clearly apparent in the peaks at 667 cm^{-1} and 2379 cm^{-1}, both of which occur on the high frequency shoulders of the true absorption and both of which increase in intensity much more rapidly than the true absorption, as is evident from a comparison of the spectra of thin and thick films (Figs. 2 and 3).

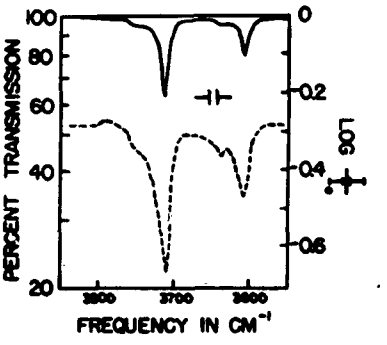

FIG. 5. The infrared spectrum of crystalline CO_2 at −190°C in the vicinity of $\nu_1+\nu_3$ and $2\nu_2+\nu_3$.

CONCLUSIONS

The spectrum of crystalline carbon dioxide agrees with the theoretical expectations. It is complicated by the presence of peaks due to $C^{13}O_2$, reflection and combination between internal and lattice vibrations. These complications are of very general occurrence and may lead to difficulties in the interpretation of the infrared spectra of crystals of more complicated molecules.

[9] D. F. Hornig and G. L. Hiebert, J. Chem. Phys. 20, 918 (1952).
[10] G. C. Pimentel, J. Chem. Phys. 19, 1536 (1951).
[11] H. Winston and R. S. Halford, J. Chem. Phys. 17, 607 (1949).
[12] L. F. Bovey, J. Chem. Phys. 18, 1684 (1950).
[13] C. Schaeffer, Z. Physik 75, 687 (1932).